FINAL TECHNICAL REPORT

Geophysical and Paleoseismic Investigation of the Cheraw Fault, Southeastern Colorado

Principal Investigators:

Mark S. Zellman and Dean Ostenaa[1]
Fugro Consultants, Inc.
1726 Cole Blvd. Ste. 230 Lakewood, CO 80214
(720) 369-8164, m.zellman@fugro.com

[1]New Address: Ostenaa Geologic LLC.
25 Grays Peak Trail, Dillon, CO 80435
(970) 389-7763, deano3geo@gmail.com

Term: January 1, 2015 to January 1, 2016

Keywords:

Paleoseismology, Quaternary geology, structure, fault characterization, seismic refraction, seismic reflection

Program Element I

U. S. Geological Survey
National Earthquake Hazards Reduction Program
Award Number G15AP000026

February 2016

Research supported by the U.S. Geological Survey (USGS), Department of the Interior, under USGS award number G15AP000026. The views and conclusions contained in this document are those of the authors and should not be interpreted as necessarily representing the official policies, either expressed or implied, of the U.S. Government.

Award G15AP000026
Geophysical and Paleoseismic Investigation of the Cheraw Fault, Southeastern Colorado

Principal Investigators:

Mark S. Zellman and Dean A. Ostenaa[1]

Fugro Consultants, Inc., 1726 Cole Boulevard, Suite 230, Lakewood, CO 80401
(720) 369-8164 phone, m.zellman@fugro.com

[1]New Address: Ostenaa Geologic LLC., 25 Grays Peak Trail, Dillon, CO 80435
(970) 389-7763 phone, deano3geo@gmail.com

ABSTRACT

The Cheraw fault is one of the few faults within the Central and Eastern United States (CEUS) known to have experienced a surface rupturing earthquake in the Holocene (Crone et al., 1997; Crone and Wheeler, 2000). Despite this unique attribute, relatively few studies have been conducted to characterize this fault. The objectives of this research are to improve the basis for seismic hazard characterization of the Cheraw fault and to identify other issues that could be resolved through further investigations. Among the major issues of uncertainty for the Cheraw fault are fault length and the relationship of the mapped scarp to older bedrock structure.

The multiple investigation methods applied in this study include: A) licensing, reprocessing, depth migration, and interpretation of two industry-collected 2D seismic reflection surveys and the review of four additional 2D time-domain seismic reflection profiles, B) collection of three new 2D p-wave shallow seismic surveys across the fault scarp, C) drilling of a shallow boring transect across the fault, D) collection of balloon-based aerial photography and generation of a high-resolution Structure from Motion (SfM) digital elevation model (DEMs) and orthophotography with Agisoft™ software, and E) mapping of surficial geology and geologic structure.

Three primary conclusions, focused on the northeast extension of the Cheraw fault, were obtained from this research: 1) The topographic scarp which characterizes the Cheraw fault, including the northeast extension, is associated with fault structure at depth which extends from the ground surface to at least 2 to 3 km depth into lower Paleozoic strata and basement, 2) The vertical offset of the basal contact of early (?) Quaternary Nussbaum Alluvium defined through geologic mapping, borehole data,

and shallow seismic surfaces at Site 1 near Haswell, CO, appears to be ~3 m; and 3) Surface displacements, and shallow structure of the Cheraw fault are not impacted by the dissolution of Permian evaporate deposits; Cheraw fault structures extend above and below the Permian units as planar structures.

The results of this study have several implications for seismic hazard characterization of the Cheraw fault. First, we estimate that the minimum rupture length appropriate for seismic hazard characterization of the Cheraw fault should be 61 km. Evaluation and analyses of seven industry seismic reflection lines shows that the dip of the Cheraw fault, into basement rocks at depths of 2 to 3 km, is ~75° which is much steeper than typical dip values used in prior seismic hazard characterizations. This research also develops new estimates of total Cenozoic and Quaternary vertical offset for the Cheraw fault which impact weights and values used in characterizing slip rate and recurrence for the fault.

TABLE OF CONTENTS

ABSTRACT I
1.0 INTRODUCTION 1
2.0 BACKGROUND 2
3.0 METHODOLOGY 7
3.1 Industry Seismic Reflection Surveys 7
3.2 Shallow Seismic Surveys 9
3.3 Boring Transect 10
3.4 Aerial Photography and Agisoft™ Structure from Motion Processing 10
3.5 Geologic Mapping 11
4.0 RESULTS AND CONCLUSIONS 12
4.1 Bedrock Structure of the Northeast Extension of the Cheraw Fault 12
4.2 Deformation of Nussbaum and Rocky Flats Alluvial Surfaces 14
4.3 Impact of Permian Evaporites 18
5.0 IMPLICATIONS FOR SEISMIC HAZARD MODELS AND FUTURE WORK 19
6.0 ACKNOWLEDGEMENTS 24
7.0 DISSEMINATION OF RESULTS 25
8.0 REFERENCES 26

LIST OF TABLES

Table 1. Estimated Vertical Fault Offsets 13
Table 2. Comparison of Existing Seismic Source Characterization Parameters and New Data Constraints for the Cheraw Fault 19
Table 3. Cheraw Fault Stratigraphic Datums, Estimated Vertical Offsets, and Slip Rates 22

LIST OF FIGURES

Figure 1. Location Map
Figure 2. Seismotectonic Setting
Figure 3. Geomorphology
Figure 4. Geologic Map and Stratigraphy
Figure 5. Along-Strike Scarp Profile
Figure 6. Line A and B: 2D Seismic Reflection Profiles
Figure 7. Line C: 2D Seismic Reflection Profile
Figure 8. Line D: 2D Seismic Reflection Profile
Figure 9. Line E: 2D Seismic Reflection Profile
Figure 10. Line F: 2D Seismic Reflection Profile
Figure 11. Haswell Area Site 1 and Site 2 Investigation
Figure 12. Site 1 Fault Interpretation
Figure 13. Site 1 Structural Map
Figure 14. Site 1 Outcrop Map
Figure 15. Photograph of Haswell Area Bedrock Fault Exposure
Figure 16. Photograph of Nussbaum Alluvium Basal Contact
Figure 17. Site 1 Shallow Seismic Refraction Survey Profile SL-01
Figure 18. Site 2 Shallow Seismic Refraction Survey Profile SL-02
Figure 19. Site 3 Shallow Seismic Refraction Survey Profile SL-03

1.0 INTRODUCTION

The Cheraw fault is located in southeastern Colorado within the Great Plains Physiographic province approximately 100 km east of the city of Pueblo (Figure 1). It is one of only a few faults within the Central and Eastern United States (CEUS) known to have experienced a surface rupturing earthquake in the Holocene (Crone et al., 1997; Crone and Wheeler, 2000). However, it has been the focus of limited detailed investigations. Published seismic source characterizations (Peterson et al., 2014; CEUS-SSCn 2012) of this fault have been based on incomplete regional-scale geologic mapping and results from a single trench which may not record a complete paleoseismic record. Questions remain regarding the relationship of the Cheraw fault to older bedrock structure, the long-term rupture history, and amount of displacement on the fault. Recent studies by Zellman and Ostenaa (2011; 2014) have provided evidence that strongly suggests a topographic scarp extending to the northeast from the northern-most point of the fault mapped by Sharps (1976) is a continuation of the previously mapped Holocene scarp of the Cheraw fault.

The goal of this research is to address major uncertainties associated with the characterization of the Cheraw fault. To meet this goal, three primary objectives are identified: 1) define bedrock structures and their relationship to the northeast extension of the fault, 2) evaluate the deformation of early (?) Quaternary deposits on the Nussbaum pediment on the northeast extension, and 3) Determine the influence that dissolution of soluble Permian evaporites has had (if any) on the Cheraw fault.

This report summarizes the results from research conducted under U.S. Geological Survey (USGS) National Earthquake Hazard Reduction Program (NEHRP) program (NEHRP) Award # G15AP00026. The study addresses Program Element 1, National and regional earthquake hazards assessments.

2.0 BACKGROUND

The Cheraw fault is a northeast trending fault with a down-to-the-northwest sense of motion. It is located in western Great Plains physiographic province of southeastern Colorado, approximately 100 km east of the city of Pueblo (Figure 2), a region generally characterized by a lack of active faults and low rates of seismicity.

The Cheraw fault is located on the western limb of the northeast plunging Las Animas Arch, a structure which overlies a basement suture zone and has experienced tectonic reactivation multiple times (Whitmeyer and Karlstrom, 2007; Tickoff and Maxson, 2001; Merewether, 1987; Rascoe, 1978). Beginning in the Proterozoic, Mazatzal terrain accreted against Yavapai terrain (Carlson, 2007). The suture zone between the terrains is recognized as a northeast trending structure within crystalline basement in southeastern Colorado and in the vicinity of the Las Animas Arch (Sims et al., 2001). The Las Animas Arch first became a positive structure in the late Paleozoic as a result of north - northwest directed regional compression during the Ouachita-Marathon Orogeny (Rascoe, 1978; Kluth and Coney, 1981), or alternatively from southwest – northeast directed regional compression as proposed by Ye et al., (1996). The Las Animas Arch experienced its second period of tectonic uplift as a result of Laramide shortening when Cretaceous rocks were warped over the broad anticline and the Denver basin subsided to the northwest (Tickoff and Maxson, 2001; Curtis, 1988) (Figure 2). The most recent period of activity is represented by down-to-the-northwest normal faulting along the Cheraw fault. The focal mechanism solution (Herrmann, 2009) from a 2009 M 3.9 earthquake about 40 km east-northeast of the fault (Figure 2) confirms the existence of contemporary extensional stress regime in the region with northwest-southeast oriented minimum horizontal stress axis, consistent with contemporary reactivation of arch-parallel structure as normal faults.

Geomorphic mapping shows that the surface trace of the Cheraw fault extends for at least 59 km, (Zellman and Ostenaa, 2014) (Figure 3). The fault was originally identified and mapped by J.A. Sharps in 1968 and described by Scott (1970) (Kirkham and Rodgers, 1981). Sharps (1976) described a ~45 km long fault trending N45°E as an inferred structure cutting the Upper Cretaceous Smokey Hill Shale Member of the Niobrara Formation (Fm.), and concealed beneath Quaternary alluvium (Holocene), loess (Holocene and Pleistocene), slopewash (Holocene), and lower Rocky Flats Alluvium

(Pleistocene) deposits (Figure 4a). A possible northeast extension of the fault has been discussed at least since Kirkham and Rodgers (1981) recognized that the characteristic topographic scarp associated with the mapped trace (Sharps, 1976) extends to the northeast. Their map extended the fault to the northeast trending ~N65°E from the northern end of the Sharps (1976) to a point just to the southwest of Haswell. However, the Kirkham and Rodgers (1981) extended fault length was never included in subsequent map depictions. More recent evaluations using USGS National Elevation Dataset (NED) 10-m digital elevation model (DEM) data have allowed extension of the scarp further northeast of Haswell (Zellman and Ostenaa, 2014).

Prior investigators have recognized the relatively limited offset associated with the Cheraw fault, but have not defined the relative amounts of displacement over time. The total vertical throw of the fault has remained similarly unknown, however the total vertical throw is constrained to less than 150 to 215 m, the estimated thickness of Smoky Hills Member of the Niobrara Formation in the vicinity of the Cheraw fault because neither the underlying Fort Hays member of the Niobrara Fm. or overlying Pierre Shale are juxtaposed at the surface against the Smoky Hills shale along the fault (Figure 4a) (Crone et al., 1997). Sharps (1976) used oil and gas well logs to develop structure contours for the top of the Dakota Fm. and estimate a maximum of 6 to 8 m of vertical displacement across the fault (Crone et al., 1997; Crone and Wheeler, 2000). Zellman and Ostenaa (2011 and 2014) evaluated a more recent database maintained by the Colorado Oil and Gas Information System (COGIS), created 3D surfaces, and cut profiles on the top of the Dakota Fm. to assess potential offset of this datum. That evaluation suggested that a maximum vertical displacement of the Dakota Fm. is probably less than about 50 m. Although the current well data are more abundant than what was available for Sharps (1976), the well data are still sparse, with significant uncertainties in the resulting estimates of displacement due to large well spacings, potential issues with formation top reporting, and irregularity in the surface due to solutioning of underlying units. Kirkham and Rodger (1981) reported that the early Quaternary Rocky Flats alluvium is offset up to 12 m across the fault. Crone et al. (1997) suggested up to 7 to 8 m of offset of Rocky Flats alluvium, apparently based on topographic profiles, but documented only 3.2 to 4.1 m of bedrock offset from trenching and boring profiles at a site where the surface scarp height is 3.6 m.

The defining characteristic of the Cheraw fault is a subtle, yet distinct, northwest-facing scarp which forms a gradient barrier for the local drainages flowing across the southeast-sloping regional drainage, and an obstruction to southeast-directed prevailing winds (Kirkham and Rodgers, 1981; Crone and Machette, 1995 and Crone and Wheeler, 2000) (Figure 3 and 4a). Erosion of the relatively soft Cretaceous bedrock units, and the partial burial of the scarp by eolian deposits and locally ponded alluvium, contribute to the subtle appearance of the scarp and an appearance of being a much older feature than it is known to be (Crone and Wheeler, 2000). Along the base of the scarp, vegetation lineaments and numerous closed depressions that intermittently hold water form a clearly visible alignment on topographic maps, DEM derivative slope, aspect, and hillshade maps, aerial photography, and multispectral imagery. Although the scarp is subtle, an along-strike profile (Figure 5) shows a consistent morphologic expression for its entire 59 km length. The scarp is visible in all surfaces and all ages of material it intersects, with the possible exception of Holocene alluvium in floodplains and terraces adjacent to streams. Preliminary topographic profiles of the NED 10-m DEM at locations along the length of the scarp, show typical scarp heights of ~3 to 5 m. Scarp heights up to ~10 to 12 m have been observed, but these sites require confirmation through further analysis. Our preliminary analyses show no consistent correlation between areas of higher apparent scarp height and areas of older geomorphic surfaces.

At three locations along the scarp, pediments and alluvium of early (?) Quaternary Nussbaum and Pleistocene Rocky Flats ages are transected and offset by the fault (Figures 3, 4a, and 5). The pediments are mantled with thin alluvium (the Nussbaum Alluvium and the Rocky Flats Alluvium), and covered with variable thickness of younger eolian deposits. The Nussbaum pediment is not directly dated, but fossils from the type locality north of Pueblo (~ 100 to 120 west of the Cheraw fault) and from gravel pits in Morgan and Logan Counties suggest an early Quaternary, or possible late Pliocene age (Scott, 1963, 1965, 1975, 1982). Schildgen et al. (2002) assigned an age of 1.35 Ma to the Rocky Flats pediment surface near Boulder based on soil profile development described by Birkeland et al. (1999), and thus by inference dated the Nussbaum surface as >1.35 Ma. If these ages apply to the mapped pediments cut by the Cheraw fault, these sites should provide a robust long-term record of slip for the Cheraw fault.

Mapping and correlation of the Nussbaum and Rocky Flats pediments has relied for the most part on the relative geomorphic position of the pediments and thin overlying alluvium units above stream grade, and their inset relations. Only a few investigations describing the relationships and ages of the overlying alluvial and eolian cover on these older surfaces in eastern Colorado have been published, although it is long recognized that these units must have a composite history (e.g., Scott, 1975). More than 120 km north of the Cheraw fault, extensive trenching and dating on the Anton Escarpment by Noe (2010), shows the complex history of erosion and deposition associated with this large geomorphic feature in this setting, which apparently formed primarily since about 30 ka. Work along the Front Range north and west of Denver (Riihimaki, et al., 2006; Duhnforth et al., 2012; and Foster et al., 2013, 2014) suggests that the Rocky Flats and Nussbaum surfaces may have been established long ago, but abandonment ages are much younger (by up to orders of magnitude) than previously suspected and that no single age may be appropriate for both the basal alluvium and overlying deposits and geomorphic surfaces. Work on both the Anton Escarpment and the northern Front Range surfaces indicates that the erosional and depositional history of the High Plains has been much more dynamic than implied by early age models linked to base level fall on the master streams. For the Cheraw fault evaluations, the implication of these studies is much greater uncertainty in the potential range of ages for older alluvium and geomorphic surfaces mapped as Nussbaum and Rocky Flats.

Closed depressions are common features in southeastern Colorado, and an alignment of these features is coincident with the surface trace of the Cheraw fault (Kirkham and Rodgers, 1981). Note the many small depressions along the northeast side of the fault in Figure 3. Closed depressions are also scattered on pediment surfaces capped with Quaternary alluvium (Sharps, 1976; Walker, 1985). They occur in a range of sizes from 10’s of m to 1000’s of km in width. The origin of the depressions is poorly understood due to a lack of detailed study. Possible genesis of these features include topographic enclosure due to faulting, eolian deposition and deflation, local subsidence along the fault due to shallow dissolution of Niobrara Shale, and subsidence due to large scale dissolution of deeper Permian evaporites (Walker, 1985; White, 2012). A prominent northwest-southeast alignment of three very large closed topographic depressions intersects the Cheraw fault at the far eastern end of the fault (Figure 3). These depressions are much larger than the small depressions and are thought to be caused by the dissolution of Permian evaporite units (Walker, 1985; White, 2012). The Permian

evaporites are brought closer to the ground surface in the core of the Las Animas anticline and fractures and faults are thought to act as conduits which bring water into contact with the soluble evaporite strata (Walker, 1985). Along with extensive eolian activity in the region, the continued evolution of these depressions creates significant additional uncertainty for evaluation of the offset history of the fault based on geomorphic profiles. The presence of the Permian evaporates in the subsurface, and ongoing solution activity also raises the question of possible linkage of the Cheraw fault to larger scale dissolution and thinning of that section in the subsurface.

In the only detailed paleoseismic study of the Cheraw fault, Crone et al. (1997) excavated soil pits, drilled a shallow borehole transect, and excavated a 110 m long trench (see Figures 4a and 5 for location). The trench was sited within an abandoned channel of inferred late Pleistocene age inset within remnants of much older Rocky Flats alluvium, and earthquake timing was determined through thermolumenisence (TL) and radiocarbon dating. The trench exposure identified three events that occurred since ~20 to 25 ka, with the best estimate for the age of the most recent event of 8 ka (Crone et al., 1997). Based on their age of the oldest faulted deposits (20 to 25 ka) and the offset of those deposits (~3.2 to 4.1 m), latest Pleistocene-Holocene slip rates may be in the range of 0.13 to 0.21 mm/yr. The oldest faulted deposits on the footwall in the trench are fluvial deposits, which occupy the late Pleistocene abandoned channel. These deposits were not dated during the Crone et al. (1997) study because charcoal was absent and at the time TL was not effective at dating these type of deposits (S. Mahan, personal communication, April 9, 2015). Based on the inferred geomorphic age of the late Pleistocene channel, Crone et al. (1997) suggested that the Cheraw fault was inactive from 20 to 25 ka to ~100 ka or older. However, Crone and Machette (1995) and Crone et al. (1997) note that offset off nearby Rocky Flats alluvium may be only 7 to 8 m. Crone et al. (1997) suggest the long-term behavior of the Cheraw fault may be characterized by long periods of inactivity punctuated by relatively short episodes of seismic activity, similar to other CEUS faults such as the Meers fault. Thus, the estimated recurrence intervals may only apply to the fault during its active phases (Crone et al., 1997).

3.0 METHODOLOGY

Multiple investigation methods were applied in this study. These included: A) licensing, reprocessing, depth migration, and interpretation of two industry-collected 2D seismic reflection surveys and the review of four additional 2D time-domain seismic reflection profiles, B) collection of new 2D p-wave shallow seismic surveys across the fault scarp at three locations, C) drilling a shallow boring transect, D) collection balloon-based aerial photography and generation of a high-resolution Structure from Motion (SfM) digital elevation model (DEMs) and orthophotography with Agisoft™ software, and E) mapping of surficial geology and structure.

3.1 Industry Seismic Reflection Surveys

Multiple seismic reflection surveys collected for oil and gas exploration on the Las Animas Arch cross the Cheraw fault. In preparation for this study, ten time-domain, 2D seismic reflection profiles were previewed, and several were selected as candidates for licensing and further analysis based on data quality and clarity of fault structure. For this study, six of those previewed lines were obtained and used in the subsurface characterization of the Cheraw fault (Figure 4a). Two of these lines (Lines A and B) (Figure 4a) were licensed for use from Conoco Phillips, reprocessed, depth migrated, and interpreted in IHS Kingdom™ (Kingdom) software (Version 2015). Four additional seismic surveys (Lines C-F) (Figure 4a) were provided by and licensed from Seismic Exchange Incorporated (SEI) for use as graphical images of time-domain profiles. Seismic Lines A and B were reprocessed by Eskaton Seismic, Inc. using the following basic sequence: Geometry QC, refraction statics, noise attenuation, deconvolution, residual statics, and poststack time migration. The reprocessed time-domain profiles were then depth migrated by Dr. Morgan Brown of Tenax Geoscience LLC. The prestack depth migration process involved the construction of an interval velocity model and cross-checking result with geologic formation top depth picks from COGIS (2015), followed by migration with a reverse time depth migration algorithm. The remaining four time-domain profiles that were previewed provided additional constraints for the characteristics of the fault outside the area of the northeast extension, the principal focus of this study.

The 2D post stack depth migration (PSDM) files for Lines A and B were loaded into the Kingdom project file for interpretation, analysis, and mapping of formation tops and structural features. The emphasis of mapping was directed towards the upper ~900 m of profile and away from the edges to avoid areas where the processed data can be less reliable. In addition to the PSDM files, the other data added to the Kingdom project include well locations and formation tops obtained from COGIS (2015) and the Sharps (1976) geologic map. Approximate geologic formation tops ranging in age from Cretaceous to Mid-Mississippian were attributed to reflectors based on formation top depth picks projected onto the seismic profiles from wells within 5 km and from stratigraphy presented by Merewether (1987) for the Las Animas Arch (Figure 4b). Stratigraphic units older than Mid-Mississippian St. Genevieve Fm., including crystalline basement, were not assigned to reflectors (Figures 6a and 6b) because very few wells in this area penetrate below the Mid-Mississippian depth range. As a result, there is a lack of reliable depth picks from wells for deeper units. For Lines A and B seismic profiles the depth to basement is estimated to be ~2000 m below ground surface based on basement contours shown in Hemborg (1996). Fault mapping on the 2D seismic data consisted of the delineation of a single primary active structure, the Cheraw fault, and other older selected faults. Faults are mapped as solid lines where strong evidence such as offset, truncated, or warped reflectors support their presence. Dashed lines are applied to faults whose presence is inferred. Faults are mapped through Permian evaporate horizons into lower Paleozoic units to the point where each fault becomes indiscernible due to resolution or structural complexities. The upper-most location of the Cheraw fault in each of the seismic reflection profiles was integrated into a Geographic Information System (GIS) for the purpose of comparing its location with the topographic scarp (Figure 4). The Cheraw fault's apparent vertical offset was determined by measuring the vertical separation of prominent reflectors with known ages in depth migrated profiles.

The additional 2D time-domain seismic profile image files (Lines C-F) (Figures 7 to 10) are graphical, which prevents them from being integrated into the Kingdom project file and interpreted with the depth corrected seismic profiles (Lines A and B). Instead, they were printed and interpreted graphically. Prominent reflectors from the depth-migrated data were identified based on similarity of reflectors seen in depth migrated Lines A and B (Figures 6a and 6b). Faulting was mapped, and the position of the Cheraw fault, nearest to the surface, was incorporated into the GIS analysis based on shot-points that are not shown because of stipulations in the data licensing agreement.

The industry-collected 2D seismic reflection surveys (Figures 6 to 10) were not collected perpendicular to fault strike. Therefore, the dip of the fault shown in each image is apparent. The true dip of the Cheraw fault was calculated for depth migrated seismic lines A and B (Figures 6a and 6b) by first measuring the apparent dip and then correcting for true dip based on the angle between the seismic line and the projected fault plane (i.e. topographic scarp). Dip was not calculated for the time domain seismic lines (Lines C-F). Rather, they were used as a relative check, and in all cases they agree with the depth migrated data and support the observation of a steeply dipping Cheraw fault.

3.2 Shallow Seismic Surveys

Shallow seismic surveys (SL-01, SL-02, and SL-03) were collected at three sites on the Cheraw fault (Figures 4, 5, and 11) to characterize the fault and adjacent shallow subsurface stratigraphy. Two of the survey sites (Site 1 and Site 2) are located on the scarp over Nussbaum Alluvium, the primary features which defines the northeast extension of the Cheraw fault. The third site (Site 3) is near the central part of the fault on the scarp over Rocky Flats Alluvium. The shallow seismic data was collected using a 24-channel (92 m long), DQA Link-2 seismograph with radio trigger system, and 12 lb. sledge hammer and aluminum strike plate source. The shot/receiver spacing was 4 m. Additional shot points were located at 24 m, 16 m and 8 m on the hanging wall (west / northwest) side of each line and 16 m and 24 m on the footwall (east / southeast) side of each line. Because the fault scarp is longer than a single 92 m long spread, multiple overlapping aligned seismic surveys were collected at each site. At Site 1, a 12 channel overlap was applied to all three lines which comprised SL-01 to ensure maximum data coverage in the seismic line overlap zones. At Site 2 a 6 channel overlap was applied to SL-02 and at Site 3 a 6 channel overlap was used for SL-03. Each 2D seismic line was oriented approximately orthogonal to the local fault strike based on the orientation of the topographic scarp. The coordinates for all shot point and receivers were collected with a Trimble Juno GPS paired with an external Trimble ProXH antenna. P-wave refraction profiles were processed by FCL using Rayfract software.

3.3 Boring Transect

A boring transect consisting of 4 borings was drilled at Site 1 (Figure 11) for the purpose of determining the depth to the top of rock, to characterize the alluvium and bedrock substrate, and to calibrate the analysis of the seismic reflection profiles. The profile was oriented approximately orthogonal to the scarp along a bearing of N15°W. At each boring location a 3.25-inch inside diameter (ID) hollow stem auger (HSA) was advanced through Nussbaum Alluvium until Niobrara shale bedrock was confirmed. Standard Penetration Tests (SPT) were completed using a 2.0-inch outer diameter (OD) split-spoon with catcher at intervals of 2.5 feet. The coordinates for all borings was collected with the paired Trimble Juno GPS and ProXH antenna.

Boring locations and depth to bedrock were added to a topographic profile and used to estimate the apparent vertical offset of the base of the alluvium / top of bedrock across the projection of the Cheraw fault.

3.4 Aerial Photography and Agisoft™ Structure from Motion Processing

High resolution structure from motion (SfM) orthoimagery and digital elevation models (DEMs) were produced for the Site 1 field area near Haswell (Figure 11) to provide basemaps for geologic mapping and elevation control for geologic profiles and analysis. Working under the direction of Dr. Edwin Nissen, Colorado School of Mines (CSM) graduate students Kendra Johnson and Lia Lajoie used a helium balloon based platform (as described in Johnson et al. 2014) to collect aerial photos over the 0.15 km^2 Site 1 area. The photographs were processed using Agisoft™ software to produce high-resolution SfM orthoimagery and DEMs with <20 cm grid cell resolution. The mosaicked orthophotos and DEMs were georeferenced based on ground control points whose position was established with a Trimble GeoExplorer GPS with and a referenced to a local USGS benchmark (HAS).

Agisoft™ was also used to process a 3D photo-mosaic of the vertical outcrop exposure of Niobrara shale at Site 1 to serve as a high-resolution basemap for geologic and structural mapping.

3.5 Geologic Mapping

Geologic structures and bedding contacts exposed in the bedrock outcrops were mapped in the field to document fault-related deformation and to constrain the location of the Cheraw fault. At Site 1 near Haswell (Figure 11), the Smoky Hill Member of the Niobrara Fm. is exposed in a vertical outcrop and on the ground surface within an eroding landscape. Faults, joints, and bedding orientations were measured using a Brunton™ pocket transit set to a declination of 7.36°E +/-0.35°, and the insitu basal contact of the Nussbaum Alluvium was mapped where it is naturally exposed. All measurement and observation points were collected using a handheld Garmin™ GPSmap 62 Global Position System (GPS) unit. The mapped information was overlain in GIS onto SfM DEM and orthoimage basemaps created with Agisoft™.

4.0 RESULTS AND CONCLUSIONS

The results of this study support three broad conclusions as follows: 1) The topographic scarp which characterizes the Cheraw fault, including the northeast extension, is associated with fault structure at depth which extends from the ground surface to at least 2 to 3 km depth into lower Paleozoic strata and basement, 2) The vertical offset of the basal contact of early (?) Quaternary Nussbaum Alluvium as defined through geologic mapping, borehole data, and shallow seismic surveys at Site 1 near Haswell, CO, is very limited; and 3) Surface displacements, and shallow structure of the Cheraw fault are not impacted by Permian evaporate deposits. Cheraw fault structures extend above and below the Permian units as planar structures.

4.1 Bedrock Structure of the Northeast Extension of the Cheraw Fault

Interpretations made from two depth-migrated (Lines A and B) (Figures 6a and 6b) and four time-domain (Lines C-F) (Figures 7-10) 2D seismic reflection profiles clearly show the Cheraw fault is a structure in bedrock that extends into lower Paleozoic units before becoming obscured by limited data resolution. In each seismic profile, the up-dip projection of this structure is spatially correlative with the 59-km-long topographic scarp which characterizes the Cheraw fault, including the northeast extension (Figure 4a). The time-domain profiles (Figures 7-10) suggest similar characteristics both on the northeast extension and the previously recognized portion of the fault mapped by Sharps (1976).

The depth migrated seismic data profiles (Lines A and B) (Figure 6) show reflectors with well ties and stratigraphic picks from the ground surface to depths of ~2000 to 2300 m (6000 to 7000 ft on Figure 6). This interval includes Cretaceous to Paleozoic sedimentary rocks over crystalline basement (Figure 4b). Deeper reflectors, imaged on both profiles, suggest continuation of the Cheraw fault into basement (?) rocks and to depths of at least ~2500 to 3000 m (8000 to 10000 ft on Figure 6). The time domain seismic profiles (Lines C-F) (Figures 7-10) show a similar stratigraphic interval over a similar depth. The strata imaged in the reflection data record at least three periods of deformation, Paleozoic during the formation of the Ancestral Rocky Mountains (Kluth and Coney, 1981; Ye et al., 1996), Late Cretaceous to Early Cenozoic during the Laramide Orogeny (Tickoff and Maxson, 2001), and Neogene to modern northwest-southeast extension (Herrmann, 2009; Levandowski et al., In Review).

Analysis of the apparent vertical offset of prominent reflectors across the Cheraw fault identifies at least two clear styles of faulting (Table 1). In both Lines A and B, the depth migrated 2D seismic reflection data indicate a steep, planar, apparently dip-slip fault, dipping ~75° to depths of 2 to 3 km. Along this discrete fault break we observe ~24 to 30 m of apparent vertical offset in upper Cretaceous units within a narrow zone proximal to the fault (near fault in Table 1). In Line B, which appears to lie closer to the center of the main fault structure, vertical offset is larger, and increases significantly in pre-Cretaceous units. Across a broader zone of tilting, folding, and faulting (far field in Table 1), vertical offsets are ~50 to 100 m in upper Cretaceous units and ~60 to 160 m in mid-Cretaceous to older Mesozoic and Paleozoic units. Again, there is possibly more offset, and more complex structure, particularly in the deeper strata, in Line B which lies to the south. These results from the depth-migrated seismic sections are in accord with the <50 m of vertical offset for the top of the Dakota Fm. Initially estimated by Zellman and Ostenaa (2011, 2014) based on the sparse data in the Colorado Oil and Gas Information System (COGIS).

Table 1. Estimated Vertical Fault Offsets

Seismic Line	Reflector Group	Formation	Near-fault Vertical Offset*	Far-field Vertical Offset*	FF Residual (FF-NF)
			meters	*meters*	*meters*
Line A	A	Greenhorn	24	46	21
		Dakota	24	58	34
		Morrison	24	58	34
	B	Blaine	24	67	43
		Virgil	*unresolved*	79	*unresolved*
	C	Morrow	*unresolved*	82	*unresolved*
		St. Genevieve	*unresolved*	107	*unresolved*
Line B	A	Greenhorn	30	98	67
		Dakota	*unresolved*	*unresolved*	*unresolved*
		Morrison	61	98	37
	B	Blaine	61	104	43
		Virgil	76	116	40
	C	Morrow	*unresolved*	159	*unresolved*
		St. Genevieve	*unresolved*	107	*unresolved*

Notes: *Near-fault offsets are measured from projections of offset reflectors across a zone up to ~250 m wide for Lines A and B. Far-Field offsets are measured across a zone up to 2 km wide for Line A and 1 km wide for Line B.

Time domain images from four other 2D reflection lines (Figures 7-10) do not provide specific estimates of fault offset but do show characteristics that are consistent with those seen in the depth

migrated data from Lines A and B (Figure 6). In all lines, including those on the main section of the Cheraw fault, there appears to be a relatively narrow, steep, and planar fault which is superimposed on a broader, more complex deformation zone with overall larger total offset.

During the Paleozoic the Ancestral Rocky Mountains and nearby Las Animas Arch experienced uplift as a result of regional compression. This period of deformation is recognized in the seismic data as faulting, and by reflectors that show a greater degree of tilting and folding than is observed in the overlying younger units. The Paleozoic faults are best seen in Line A (Figure 6), to the northwest of the Cheraw fault, or left half of the figure. These faults are steeply dipping and exhibit apparent vertical offset in the seismic data, sometimes both up and down along the same fault, which suggests a component of lateral offset. The strike of these faults is unknown because they are not recognized any other seismic profile included in this study. The most prominent Paleozoic-related fold is observed in both Lines A and B (Figure 6) in the footwall of the Cheraw fault, and in close proximity to the fault. In both profiles, the forelimb is intersected by the Cheraw fault, and the back-limb extends to the southeast towards the axis of the Las Animas Arch. The up-section limit of this fold is interpreted to be no younger than the Blaine Fm. with the largest growth having occurred sometime in the Mid-Late Pennsylvanian.

Post-Paleozoic deformation includes northeast directed Laramide shortening and modern northwest-southeast extension which is reflected in the seismic profiles (Figure 6) as broadly warped Mesozoic strata and apparent vertical offsets across the Cheraw. Besides activity of the Cheraw fault during this timeframe, subtle warps and apparent truncations are observed in Mesozoic strata, through at least the Greenhorn Fm., overlying the near-vertical Paleozoic faults (Figure 6: Line A and possibly Line B), suggest a reactivation phase of these faults.

4.2 Deformation of Nussbaum and Rocky Flats Alluvial Surfaces

Deformation of the Nussbaum Alluvium was evaluated at Sites 1 and 2, adjacent to the town of Haswell, CO (Figures 3, 11, 12) where the Cheraw fault scarp intersects the western edge of a pediment surface capped with early(?) Quaternary Nussbaum Alluvium. The field investigation at Site 1 applied shallow seismic surveys, a shallow borehole transect drilled in to the top of bedrock, aerial photo collection and SfM image and DEM processing, and geologic and structural mapping (Figure

13) to constrain the zone of faulting and estimate the apparent down-to-the-northwest vertical offset on the base of the Nussbaum Alluvium (Figure 11). At Site 2 only shallow seismic survey methods were applied to locate the fault and constrain vertical offset.

The only identified bedrock exposure along the entire Cheraw fault scarp exists at Site 1 (Figures 13 and 14) where bedrock is exposed on the ground surface and in a vertical outcrop exposure. In the outcrop (Figure 14), Smoky Hills Member of Niobrara Fm., consisting of shale and thin beds of limestone, is exposed in a near-vertical outcrop exposure and in scattered outcrops on the ground surface. On the eastern edge of this area, and near the highway to the north, are multiple exposures where the shallow-dipping basal contact of bedded Nussbaum Alluvium overlies Niobrara Fm. (Figures 12 and 13).

We used the detailed images output from Agisoft™ (Section 3.4) for mapping of the vertical bedrock outcrop of Niobrara Fm. (Figure 14) including the delineation of small displacement faults (~5 to 10 cm vertical offset), the tops of prominent bedding, and “plates” of $CaCo_3$ (?) mineralization. Bedding attitudes and fault orientation are marked at their observation points. The overall outcrop ranges in height from ~3 to 4 m and measures ~60 m from end to end. The west side of the outcrop (right) is characterized by three intervals of slopes and ledges created by alternating exposures of shale and limestone, and the east side (left) is characterized by less prominent bedding as a result of a thicker interval of shale. Two areas near the center of the outcrop are deformed, as expressed by warped bedding. In both cases, the deformation is separated from the adjacent gently dipping beds by small displacement faults which intersect the outcrop at high angles. In at least one location in the center of the outcrop, the large “plates” of mineralization are connected, and directly associated with faulting. Prominent beds and a characteristic marker bed that are clearly visible on the west side of the outcrop are not visible on the east side. These two areas of different bedding characteristics are separated by a zone ~10 m in width where the bedrock exposure is completely covered with a drape of colluvium and vegetation. This location is inferred to be the location where a main of the trace Cheraw fault intersects the outcrop marked with an orange star in Figures 12, 13 and 14.

Approximately 30 to 40 m northeast of the interpreted fault zone in the vertical outcrop, within an area of low relief and scattered bedrock outcrops (Figures 12 and 13), a thin, vertical fault was observed

juxtaposing beds dipping steeply in opposite directions (Figures 13 and 15). The fault strikes ~N60°E, which projects southwest to the major features inferred in the near-vertical bedrock outcrop and is parallel-subparallel to the orientation of the topographic fault scarp further southeast (Figures 11 and 12).

The Site 1 exposures of Nussbaum Alluvium are characterized by weak to moderately cemented coarse sand and fine rounded gravel and a planar basal contact (Figure 16). These observations are consistent with descriptions by Scott (1963, 1965, 1975) and Soister (1967) who described the basal units of the Nussbaum Alluvium at other locations to the west in the Arkansas River basin. On a transect along contour ~1380 m in the mapping area, this contact was observed in multiple natural exposures until a point when the exposure became obscured by a mantle of soil and vegetation (Figures 12 and 13). This termination aligns on a northwest strike with bedrock features and faults described above. The next observation of the basal contact was at a point ~150 m to the north-northwest in the sidewall of a wide ditch excavated sub-parallel to Highway 96. The elevation of the contact at this location is ~1376 m, approximately 3 m lower than the last observation to the south (Figure 12).

The borehole transect drilled at the northeastern edge of the Haswell site, on top of the Nussbaum surface (Figures 11, 12, and 17), encountered thick alluvium and eolian units overlying bedrock (Smoky Hill Member of Niobrara Fm.) in each of the 4 boreholes. The alluvium and eolian units consists of silt, quartz-rich fine to coarse sand and fine gravel with variable levels of cementation (mostly weak). The top of bedrock was encountered between depths of 10.1 m and 13.4 m below ground surface and is often completely weathered to clay.

Shallow seismic survey SL-01 was collected adjacent to the boring transect (Figures 11, 12, and 17) and provides data which extends the borehole interpretation. The seismic profile shows that the top of rock is associated with the ~1100 to 1300 m/s iso-velocity horizon. The apparent fault zone is between receiver stations ~133 and ~139 (Figure 17) and is characterized by a low velocity anomaly at depth and as an inflection of velocity contours at shallow depths. A large inflection of the velocity contours is observed near the northwest end of the line near station 106 (Figure 17). This is not interpreted as a

fault because it does not necessarily correlate with a low velocity zone at depth, and because of its proximity to the edge of the survey where data can be less reliable.

A profile (Figure 17) constructed by overlaying the borings with depths to top of rock, and shallow seismic profile SL-01 onto SfM derived topography places the fault between Borings 2 and 3, about mid-way up the topographic scarp, with ~3 m of vertical down-to-the-west offset on the base of Nussbaum Alluvium / top of bedrock. As shown on (Figures 11 and 12), this offset aligns along the same strike with other features described above.

Seismic survey SL-02 (Figures 11, 12, and 18) was collected at Site 2 about 300 m to the east-northeast of Site 1. The P-wave refraction profile from this survey (Figure 18) shows very similar results as those from SL-01. The interpreted fault zone is between receiver stations ~240 and ~242 and characterized by a low velocity anomaly at depth and as an inflection of velocity contours at shallower depths. Boreholes were not drilled at this location, but due to its close proximity and similar setting we interpret the top of bedrock to have a similar velocity at that observed at SL-01. In SL-02 the apparent vertical offset of the 1000 m/s velocity contour across this zone is ~3m.

Taken together, the results from outcrop mapping, boreholes, and interpretation of shallow seismic data at Site 1 present a consistent set of observations which suggest ~3 m of down-to-the-northwest vertical offset on the base of Nussbaum Alluvium across a constrained zone of northwest-striking deformation (Figure 12). On a broader scale, this zone of deformation aligns with, and is on trend with the mapped geomorphic scarp of the Cheraw fault to the southwest and northeast (Figure 11).

A third seismic survey was collected at Site 3 across a ~4 m scarp in Rocky Flats Alluvium (Figures 4a, 5, and 19). No boreholes were drilled at this site therefore depth to top of rock is not directly measured, but weathering and velocity conditions are assumed to be very similar to those characterized at Site 1. The interpreted fault zone is near the mid-point of the scarp between receiver stations 334 and 336 and is characterized by an inflection of relatively shallow velocity contours, similar to what is observed in SL-01 and SL-02, and an apparent ~3m offset of the ~1100 m/s iso-velocity horizon. The SL-03 (Figure 19) profile shows other low velocity anomalies and inflections that will require additional analysis to interpret.

4.3 Impact of Permian Evaporites

Permian evaporates are stratigraphically located between Pennsylvanian Virgilian carbonate rocks and the Triassic Dockum Group (Figure 4b) within the stratigraphic section underlying the Cheraw fault scarp. The existence of dissolution features thought to be related to these evaporates in southeastern Colorado (Walker, 1985; White, 2012) suggests the hypothesis that recent displacement on the Cheraw fault could be directly related to dissolution of these units. In that case, seismic reflection images would be expected to show significant differences in the characteristics of the Cheraw fault, above and below these horizons.

To evaluate this hypothesis, the approximate location of Permian evaporate deposits was identified in each 2D seismic reflection profile (Figures 6-10) based on formation top depth picks in local oil and gas wells (COGIS, 2015). The position of the Permian evaporates is shown on Figure 6; the top of the Permian is located at approximately 2,500 feet depth. The Permian units are characterized by a set of parallel discontinuous and wavy reflectors which may have deformed as a result of dissolution and is observed to often directly overlie continuous and horizontal, to sub-horizontal, reflectors. In each of the six 2D seismic reflection profile presented in this report (Figures 6-10) the Cheraw fault can be seen to cut cleanly through Permian evaporate horizons into lower Paleozoic units, to depths at least 1 km below the evaporates. As discussed earlier in Section 4.1, interpretations of the seismic reflection data strongly indicate that the present surface trace of the Cheraw fault corresponds to a relatively planar structure in depth section, which extends from the surface into Precambrian basement units. Thus, the hypothesis that recent displacement on the Cheraw fault might be related to dissolution within the Permian evaporate section is not supported.

5.0 IMPLICATIONS FOR SEISMIC HAZARD MODELS AND FUTURE WORK

The results of this research provide significant updates to the fault characterization inputs for seismic hazard models of the Cheraw fault. These updates include new data constraints on fault geometry, such as fault trace extent, fault length, and dip. This research also provides new data on the amount of Quaternary offset present on the northeast extension of the fault, and on the total late Cenozoic offset for the Cheraw fault. The evaluation of 2D seismic reflection data highlights the role of recurrent reactivation along pre-existing zones of structural weakness, with different styles of faulting resulting from changing tectonic stresses through geologic time. Our evaluation of these new data and prior work in the region indicates the need for updates to existing seismic hazard models of the Cheraw fault, with increased uncertainty in slip rate and event occurrence models due to a present lack of constraints on the ages of offset units, and paleoseismic event chronology.

Table 2 summarizes the fault characterization parameters for rupture length and fault dip from existing CEUS and USGS seismic hazard models (CEUS-SSCn, 2012; Petersen et al., 2014) along with potential updates to these characteristics driven by new data from this research. Our basis for these updates and implications of our new data for research and uncertainty estimates are discussed in the sections that follow.

Table 2. Comparison of Existing Seismic Source Characterization Parameters and New Data Constraints for the Cheraw Fault

Parameter	Data Source			
	Petersen et al., 2014	CEUS–SSCn, 2012		New data from this research
Rupture length	45 (1.0)	46 (0.8)	62 (0.2)	61 km (minimum)
Dip	50° (1.0)	50° (0.4)	65° (0.6)	75° (to 2-3 km depth)

Our geomorphic mapping of the Cheraw fault (Figures 3 and 5) shows that there is a geomorphic scarp expressed in the NED 10 m DEM data for at least 59 km along the Cheraw fault. This length is a minimum because both ends of the scarp terminate in areas of active or very young erosional or eolian landscapes which extend for several kilometers along the strike projection of the scarp. Multiple

seismic reflection lines northeast of the mapped scarp, including previewed lines not shown in this report, appear to show bedrock structure consistent with that observed along the main trace of the Cheraw fault (Section 4.1). However, because we have only evaluated in detail and have access to one of these 2D seismic lines (Line A, Figures 4a and 6), we consider the minimum structural or rupture length of the Cheraw fault to be bounded for now at Line A, for a total length of 61 km. The strong similarity of structure and offsets between Lines A and B, suggests that both lines record the same displacement history, despite the present absence of a mapped geomorphic evidence at Line A.

Because the USGS (Petersen et al., 2014) and CEUS (CEUS-SSCn, 2012) models pre-date the verification of northeast extension of the Cheraw fault, both models solely or strongly prefer the shorter map trace (Table 2) which resembles the original mapped fault length of Sharps (1976). The CEUS SSC provides weighted options for the fault parameters including two options for fault length; a 46 km length which corresponds for the original mapped extent and a 62 km length which includes the original mapped extent and a northeast extension (CEUS-SSCn, 2012). The shorter fault length is given a higher weight (0.8 vs. 0.2) indicating that it is the favored interpretation. The USGS Cheraw fault model uses only the shorter fault length. Both models include other logic branches and weighted options for rupture model, rate, and magnitude, which may be somewhat dependent on the fault length characterization. For example, both the CEUS and USGS model put most model weight on characteristic rupture models, with a strong bias (0.7 for CEUS and 0.75 for USGS) to magnitudes of 6.8 and greater. Rupture lengths associated with these magnitudes imply nearly all events rupture the full fault length. However, the new data which indicate a minimum fault rupture length of 61 km, would now be permissive of partial ruptures along strike with magnitudes in the 6.5 to 7.0 range and associated fault rupture lengths of 25 to 40 km based on normal fault regressions of Wells and Coppersmith (1994). Thus, a recurrence rate model limited to a lower magnitude range on the longer fault length could include up to 4 to 6 earthquakes during the period since 20 to 25 ka, based on the relatively small displacements (3.2 – 4.1 m total; Crone et al., 1997)) observed in the only trench along the fault to date. This hypothesis implies differences in event timing along strike, despite the relative uniformity of the geomorphic scarp height along the entire 61 km length of the fault, and the similarity of documented Quaternary offset at the Haswell (Section 4.2) and the Crone et al. (1997) trench site.

Likewise, our updated estimates for dip of the Cheraw fault, which appear to extend into basement structure at depths of 2.5 to 3 km (Section 4.1), imply a significantly steeper dip for the fault than previously modeled (Table 2). While the new data imply a much steeper dip than usually associated with ruptures on mature normal faults in the western United States, contemporary normal-fault earthquake ruptures on the Cheraw fault may be relatively new occurrences, which follow inherited structure derived from earlier tectonic stress regimes (Section 4.1 and discussion below). Thus, fault ruptures are “forced” to occur on steeper than optimal orientations. For Cheraw fault seismic hazard models, the data from research suggest that alternatives with steeper dips may need more weight than “typical” normal faults.

The USGS (Petersen et al., 2014) and CEUS (CEUS-SSCn, 2012) models also include alternatives to represent clustered faulting behavior, which in part depend on fault-specific estimates of total late Cenozoic and older Quaternary offset. This research provides several key findings which impact these estimates. Table 3 compiles new and existing offset and age estimates for several potential offset datums on the Cheraw fault along with the slip rate resulting from those combinations. This compilation highlights the extreme range of uncertainty presently associated with most of these estimates, primarily due to insufficient age control and knowledge pre-latest Pleistocene fault history on the Cheraw fault.

First, interpretation of the 2D reflection lines (Table 1) shows that total Cenozoic (i.e. post-Dakota SS) vertical on the Cheraw fault is significantly greater, by perhaps an order of magnitude, than the 6 to 8 m cited by Crone et al. (1997) and CEUS-SSCn, 2012, based on the Sharps (1976) structural contours. The 2D seismic reflection data show that the Quaternary Cheraw fault appears to be reactivating structural features inherited from prior, early Cenozoic and older, deformational events. The earlier deformation events were primarily compressional, and likely produced structures with significant lateral or oblique offsets, and steep dips. However, it is not clear from the 2D seismic data what proportion of the total Cenozoic offset amounts derived from either near-fault or far-field projections (Table 1), should be ascribed to late Cenozoic extension versus early Cenozoic compression.

Table 3. Cheraw Fault Stratigraphic Datums, Estimated Vertical Offsets, and Slip Rates

Datum	Age (ka)	Source/Type of Data/Vertical Offset (m)/Slip Rates (mm/yr)											
		Sh76, Cr97		KR81	Cr97				This study				
		Stratigraphic		Geomorphic			Trench		NF	FF	Geomorphic		Strat.
		6	8	12	6	8	3.1	4.1	30	98	9	4	3
Early Cenozoic	15000	0.0004	0.0005						0.0020	0.0065			
	5000	0.0012	0.0016						0.0060	0.0196			
Nussbaum Alluvium	3000										0.003	0.001	0.001
	1000										0.009	0.004	0.003
Rocky Flats Alluvium	2000			0.006							0.005	0.002	
	1200				0.005	0.007					0.008	0.003	
	400			0.030							0.023	0.010	
Late Pleistocene	100										0.09	0.04	
	25						0.12	0.16			0.36	0.16	0.12
	20						0.16	0.21			0.45	0.20	0.15

Notes: Sources – SH76 (Sharps, 1976); KR81 (Kirkham and Rogers, 1981); Cr97 (Crone et al., 1997). Type of Data – Stratigraphic, Geomorphic, and Trench data are structure contours, surface profiles, and exposures. NF (near fault) and FF (far field) are based on seismic reflection profiles described in Section 4.1. Age values used for datums are from sources, e.g., KR81 and Cr97, or ranges from other literature cited in text. Cenozoic datum uses estimated age range for onset of extensional tectonism.

We favor restricting late Cenozoic offset primarily to the narrow, discrete zone of faulting shown on Line A and Line B interpretations in Figure 6. In this interpretation, the broader zone of warping and tilting that extends 1 to 2 km from the main fault is seen as related to the early Cenozoic (Laramide) compressional deformation, which may have included oblique-normal motion on the steeply dipping, discrete fault as well. In this interpretation, maximum late Cenozoic vertical offset on the Cheraw fault based on seismic Line B, southwest of Haswell, would be about 30 m (Table 1). Maximum late Cenozoic offset from Line A, northeast of Haswell is 24 m, but Line A appears to be located near the end of the fault, where offset is decreasing. Note that we do not identify any Neogene or Quaternary reflectors in either seismic line, so the actual offset associated with late Cenozoic extension could be significantly less than these values. If the late Cenozoic extension faulting includes the broader zone of tilting and warping, it implies that surface offsets derived from trenching do not fully represent seismogenic fault slip, and associated seismic moment rates for the Cheraw fault need to be significantly increased to account for this unrecognized slip.

Finally, our investigations at the Haswell site suggest that total Quaternary slip, based on the vertical offset of the base of the Nussbaum Alluvium, could be no more than ~3 m (Section 4.2 and Figures 11, 12 17, and 18). This offset is significantly less than the very poorly constrained geomorphic offset (~6 +/-3 m), we would infer from topographic profiles near these locations. If confirmed through further investigations, the ~3 m offset of the base of the Nussbaum Alluvium could represent the entire offset history of the Cheraw fault possibly since 3 Ma. This finding could imply long hiatus between slip episodes, or alternatively that the three late Quaternary surface faulting events documented by Crone et al. (1997), which appear to drive the primary geomorphic expression of the present Cheraw fault, represent the total history of a young, new extensional phase of faulting. The apparent discrepancy of the stratigraphic versus geomorphic offsets may also suggest that the extensive active eolian processes along the Cheraw fault are overprinting the tectonic scarp in a way that slip estimates based on normal profiling approaches along the fault have far greater uncertainty than previously recognized. That uncertainty is compounded by the absence of local age control for most of the Quaternary deposits and surfaces intersected by the fault.

6.0 ACKNOWLEDGEMENTS

This research has been supported by the U.S. Geological Survey (USGS), Department of the Interior, under USGS National Earthquake Hazard Reduction Program (NEHRP) award number G15AP00026. The outcome of this study would not have been possible without the cooperation, generosity, and support from many individuals and organizations, and in particular the extensive internal support from Fugro Consultants, Inc. We are grateful to Dr. Morgan Brown for major contributions in obtaining seismic reflection surveys and depth migration processing, Dr. Bill Wepfer and the staff at Eskaton Geophysical for reprocessing seismic data, and SEI and Conoco Phillips for licensing seismic reflection profiles. Without their help, our detailed analysis of the seismic reflection data would not have been possible; The Miller family, the Wyckoff family, the CO State Land Board, and Kiowa County, CO, for land access. Dr. Ed Nissen and his students Kendra Johnson and Lia Lajoie for aerial image collection and SfM processing; Dr. Rich Briggs, Dr. Will Levandowski, and Chris DuRoss of the USGS for joining us in the field to review field sites and discuss the project. Finally thanks to our Fugro colleagues Jason Altekruse, Bruno Protti, Glen Adams, Jamey Turner, Dr. Dan O'Connell, and Dr. Carlos Mendoza for being generous with their time and for data collection, processing, and brainstorming, and to Jason Holmberg for producing the figures in this report.

7.0 DISSEMINATION OF RESULTS

Through March 2016, preliminary results of this research have been presented at the 2015 American Geophysical Union (AGU) Fall Meeting (Zellman and Ostenaa, 2015). USGS staff from the Golden Office (R. Briggs and C. DuRoss) accompanied us on a 1-day field visit in November 2015 to review findings and discuss future field investigation options. Results from this research have been used in requests for additional USGS and Colorado Geologic Survey funding and assistance. Future presentations are currently planned for the upcoming Paleoseismology, Active Tectonics, and Archeoseismology (PATA) conference in May 2016 (abstract submitted and accepted), the 2016 Symposium on the Application of Geophysics to Engineering and Environmental Problems (SAGEEP), the 35th International Geological Congress in August/September, 2016, and the Geological Society of America (GSA) annual meeting in Denver, September 2016.

Bibliography:

Zellman, M., and Ostenaa, D., 2015, Confirmation and Characterization of a Previously Unmapped Northeast Extension of the Cheraw Fault, Southeast Colorado, Abstract T51A-2862 presented at 2016 Fall Meeting, AGU, San Francisco, CA.

8.0 REFERENCES

Birkeland PW, Miller DC, Patterson PE, Price AB, Shorba RR., 1999, Soil-geomorphic relationships near Rocky Flats, Bounder and Golden, Colorado area, with a stop at the Pre-Fountain Formation paleosol of Wahlstrom (1948). Geological Society of America Field Trip No. 18.

Carlson, Marvin P., 2007, Precambrian accretionary history and Phanerozoic structures – Aunified explanation for the tectonic architecture of the Nebraska region, USA, Geological Society of America Memoirs; 200; 321-326.

CEUS–SSCn, 2012, Central and Eastern United States seismic source characterization for nuclear facilities: Palo Alto, California, EPRI, U.S. DOE, and U.S. NRC, [variously paged]. (Also available at http://www.ceus-ssc.com/Report/Downloads.html.).

Colorado Oil and Gas Information System (COGIS), 2015, Oil and gas well database: http://cogcc.state.co.us/. Website accessed last accessed February 26, 2016.

Crone A.J., Machette, M.N., Bradley, L.-A., and Mahan, S.A., 1997, Late Quaternary surface faulting on the Cheraw fault, southeastern Colorado: U.S. Geological Survey Miscellaneous Geological Investigations I-2591, 7p. Pamphlet, 1 oversize pl.

Crone, A.J., and Machette, M.N., 1995, Holocene movement on the Cheraw fault, SE Colorado – Another hazardous late Quaternary fault in the stable continental interior: Eos, Transactions of the American Geophysical Union, v.76, no. 46, November 7, 1995 supplement, p. F362.

Crone and Wheeler, 2000, Data for Quaternary faults, liquefaction features and possible tectonic features in the Central and Eastern United States, East of the Rocky Mountain front, U.S. Geological Survey Open-File Report 00-260.

Curtis, B.F., 1988, Sedimentary rocks in the Denver basin, in Baars, D.L., and 15 others, eds., Basins of the Rocky Mountain region – Decade of North American geology: Boulder, Colorado, Geological Society of America, The Geology of North America, v. D-2, p. 109-221.

Duhnforth, M., Anderson, R., Ward, D., Blum, A., 2012, Unsteady late Pleistocene incision of streams bounding the Colorado Front Range from measurements of meteoric and in situ 10Be, Journal of Geophysical Research, v117.

Foster, M., Duhnforth, M., Anderson, R., 2013, Young strath terraces on western High Plains record climate-paced variations in sediment supply from Colorado Front Range, Abstract, Geological Society of America Annual Meeting, Denver, CO.

Foster, M., Anderson, R., Mahan, S., 2014, Use of 10Be to deduce variations in sediment supply from the Front Range to the High Plains, with implications for generation of fill and strath terraces, Abstracts with Programs, Geological Society of America Annual Meeting

Hemborg, T., 1996, Basement Structure Map of Colorado with Major Oil and Gas Fields, Colorado Geological Survey, Map Series 30, Plate 1.

Herrmann, Robert, B.., 2009, Moment Tensor Solution. Accessed in April 2014 from website: http://www.eas.slu.edu/eqc/eqc_mt/MECH.NA/20090817002212/index.html.

Johnson, K., Nissen, E., Saripalli, S., Arrowsmith, J.R., McGarey, P., Scharer, K., Williams, P., and Blisniuk, K., 2014, Rapid mapping of ultrafine fault zone topography with structure from motion: Geosphere, v. 10, no. 5, p. 969-986, doi: 10.11130/GES01017.1

Kirkham R.M., and Rodgers, W.P., 1981, Earthquake potential in Colorado – A preliminary evaluation: Colorado Geological Survey Bulletin 43, 171 p., 3 pls.

Kluth, CF., and Coney, PJ., 1981, Plate tectonics of the Ancestral Rocky Mountains, Geology, v.9, no.1, p10-15.

Levandowski W., Zellman M., and Briggs R., (In Review), Gravitational body forces focus North American intraplate earthquakes.

Merewether, E. A., 1987, Oil and gas plays of the Las Animas Arch, southeastern Colorado: U.S Geological Survey Open-File Report 87-450D, 22p.

Noe, D., 2010, Anton Escarpment Paleoseismologic Investigation, Washington County, Colorado: U.S. Geological Survey (USGS) National Earthquake Hazard Reduction Program (NEHRP) External Grant Award Number 07HQGR0090.

Petersen, M.D., et al., 2014, 2014 update to the National Seismic Hazard Map (NSHM), U.S. Geological Survey: last accessed February 26, 2016 from the USGS website: http://earthquake.usgs.gov/hazards/2014prelim/.

Rascoe, B., Jr., 1978, Late Paleozoic structural evolution--the Las Animas arch; in, Energy Resources of the Denver Basin: Rocky Mountain Association of Geologists, 1978 Symposium, p. 113-127.

Riihimaki, C.A., Anderson, R.S., Safran, E.B., Dethier, D.P., Finkel, R.C., and Bierman, P.R., 2006, Longevity and progressive abandonment of the Rocky Flats surface, Front Range, Colorado: Geomorphology, v. 78, pp. 265-278.

Schildgen T., Dethier, D.P., Bierman, P., Caffee, M., 2002 26Al and 10Be Dating of Late Pleistocene and Holocene Fill Terraces: A Record of Fluvial Deposition and Incision, Colorado Front Range, Earth Surface Processes and Landforms, 27, 773-787.

Scott, Glenn R., 1963, Nussbaum Alluvium of Pleistocene (?) age at Pueblo, Colorado; Article 72, U.S. Geological Survey Professional Paper, C49-C52.

Scott, Glenn R., 1965, Nonglacial Quaternary of the Southern and Middle Rocky Mountains, in Wright, H.E., and Frey, D.G., ed., The Quaternary of the United States: Princeton Univ. Press, p. 243-254.

Scott, Glenn R., 1970, Quaternary faulting and potential earthquakes in east-central Colorado, Geological Survey Professional Paper 700-C.

Scott, Glenn R., 1975, Cenozoic surfaces and deposits in the southern Rocky Mountains, in Cenozoic history of the Southern Rocky Mountains: Geological Society of America Memoir 144, p. 227-248.

Scott, Glenn R., 1982, Paleovalley and geologic map of northeastern Colorado: U.S. Geological Survey Miscellaneous Geologic Investigations Map I-1378, scale 1:250,000

Sharps, J.A., 1976, Geologic map of the Lamar quadrangle, Colorado and Kansas: U.S. Geological Survey Miscellaneous Geologic Investigations Map I-944, scale 1:250,000.

Sims, P.K., Bankey, V., Finn, C.A., 2001, Preliminary Precambrian basement map of Colorado – A geologic interpretation of an aeromagnetic anomaly map, USGS Open-File Report 01-0364.

Soister, P.E., 1967, Relation of the Nussbaum Alluvium (Pleistocene) to the Ogallala Formation (Pliocene) and to the Platte-Arkansas divide, Southern Denver Basin, Colorado. U.S. Geological Survey Professional Paper 575-D, pp. D39-346.

Tickoff, B., and Mason, J., 2001, Lithospheric buckling of the Laramide foreland during Late Cretaceous and Paleogene, western United States, Rocky Mountain Geology, v.36, n1, p13-35.

U.S. Geological Survey (USGS), 2016, Quaternary fault and fold database for the United States, Accessed January 5, 2016, from USGS website: *http//earthquake.usgs.gov/hazards/qfaults/.*

Walker, Graham Thomas, 1985, High Plains Depressions in Eastern Colorado: Distribution, Classification, and Genesis, Unpublished Ph.D. Dissertation, University of Denver.

Wells, D.L., and Coppersmith, K.J., 1994, Analysis of Empirical Relationships among Magnitude, Rupture Length, Rupture Area, and Surface Displacement, Bulletin of the Seismological Society of America, v.84, p. 974-1002.

White, Jonathan L., 2012, Colorado Map of Potential Evaporite Dissolution and Evaporite Karst Subsidence Hazards: Map Discussion, Colorado Geological Survey.

Whitmeyer, S. and Karlstrom K., 2007, Tectonic model for the Proterozoic growth of North America, Geosphere, v.3, n.4, p.220-259.

Ye, H., Royden, L., Burchfiel, C., and Schuepbach, M., 1996, Late Paleozoic Deformation of Interior North America: The Greater Ancestral Rocky Mountains, AAPG Bulletin v80, n9, p1397-1432

Zellman, M. and Ostenaa, 2011, Investigation of the Cheraw fault through spatial analysis (abstract and presentation), GIS in the Rockies 2011, Denver, Colorado, 2011.

Zellman, M. and Ostenaa, D., 2014 Preliminary results from new investigations of the Cheraw fault, SE Colorado (abstract and presentation), Geological Society of American Rocky Mountain and Cordilleran Section Meeting, Bozeman, MT, May 2014.

Zellman, M., and Ostenaa, D., 2015, Confirmation and Characterization of a Previously Unmapped Northeast Extension of the Cheraw Fault, Southeast Colorado, Abstract T51A-2862 presented at 2015 Fall Meeting, AGU, San Francisco, CA.

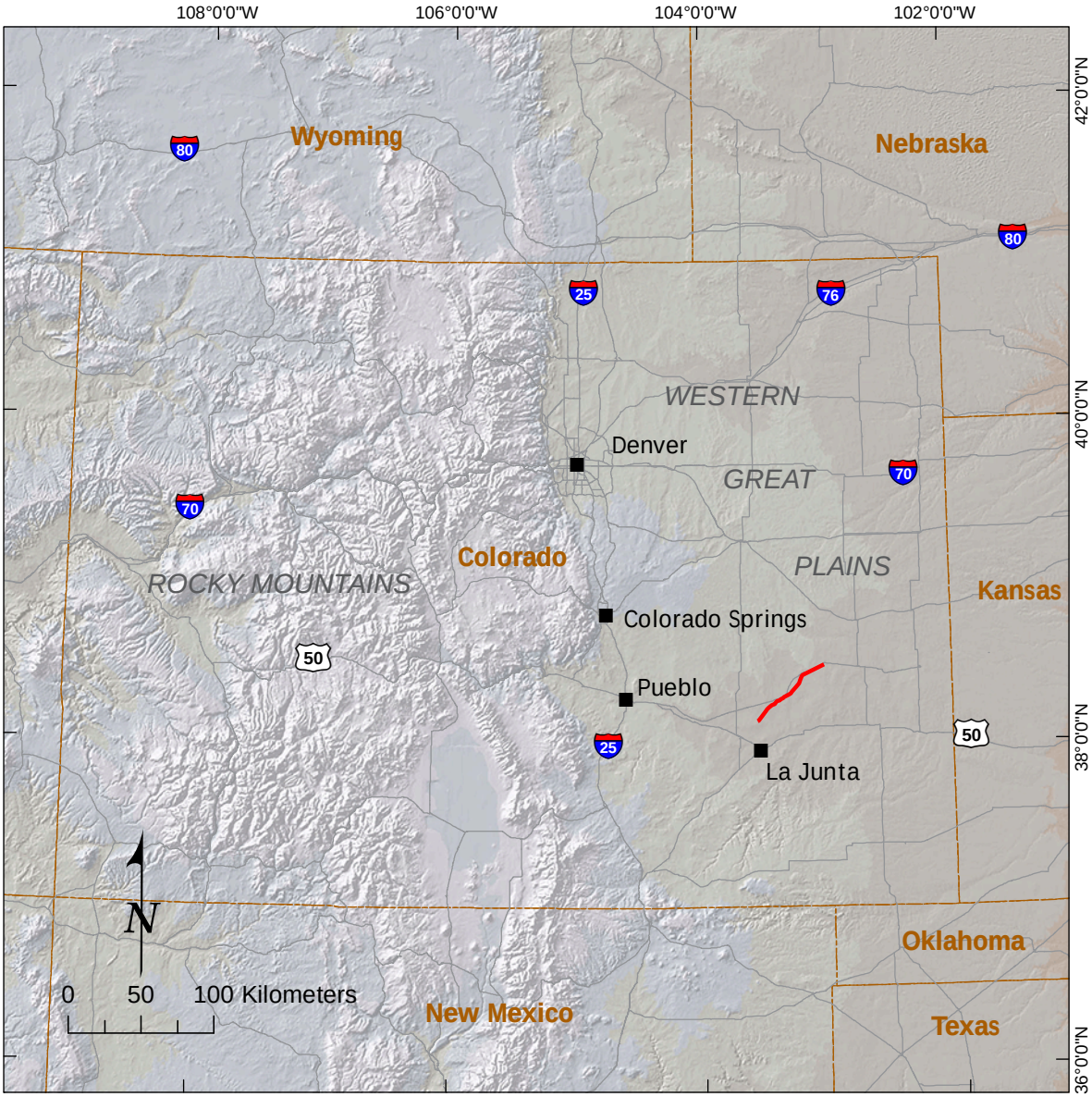

Explanation

Cheraw fault

Figure 1. Location Map

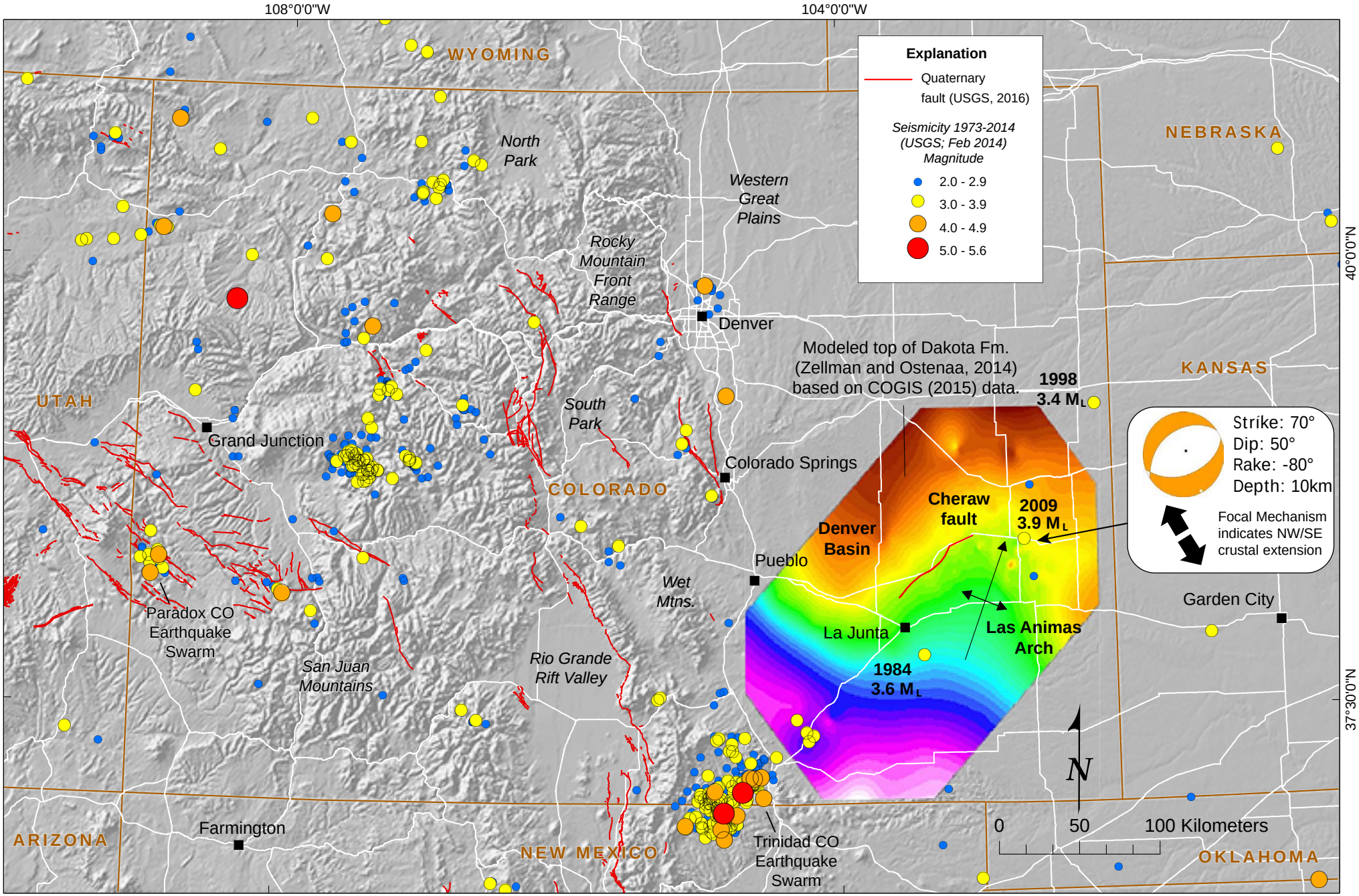

Figure 2. Seismotectonic Setting

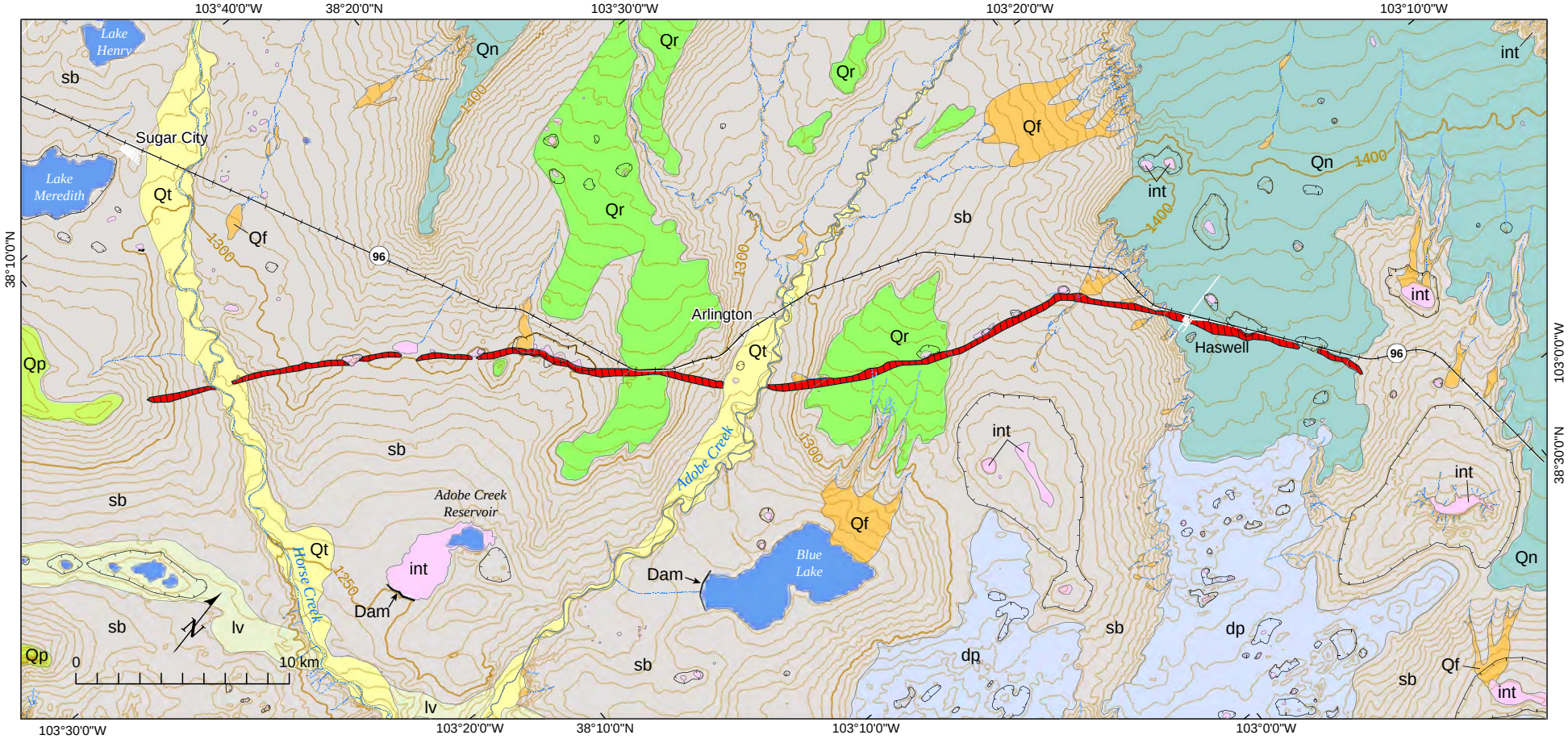

Explanation

Symbols

- Closed depression
- Railroad
- Creek or ephemeral stream
- Topographic contours (5m) USGS NED 10-m DEM

Geomorphology

- Topographic scarp (Cheraw fault)
- Water
- int — Intermittant lake
- Qt — Terrace and floodplain
- Qf — Alluvial fan

Pediment

- Qn — Nussbaum pediment (early (?) Quaternary)
- Qr — Rocky Flats pediment (Pleistocene)
- Qp — Other pediment or terrace (?)
- dp — Degraded pediment
- sb — Slope and basin
- lv — Linear valley

Figure 3. Geomorphology

A)

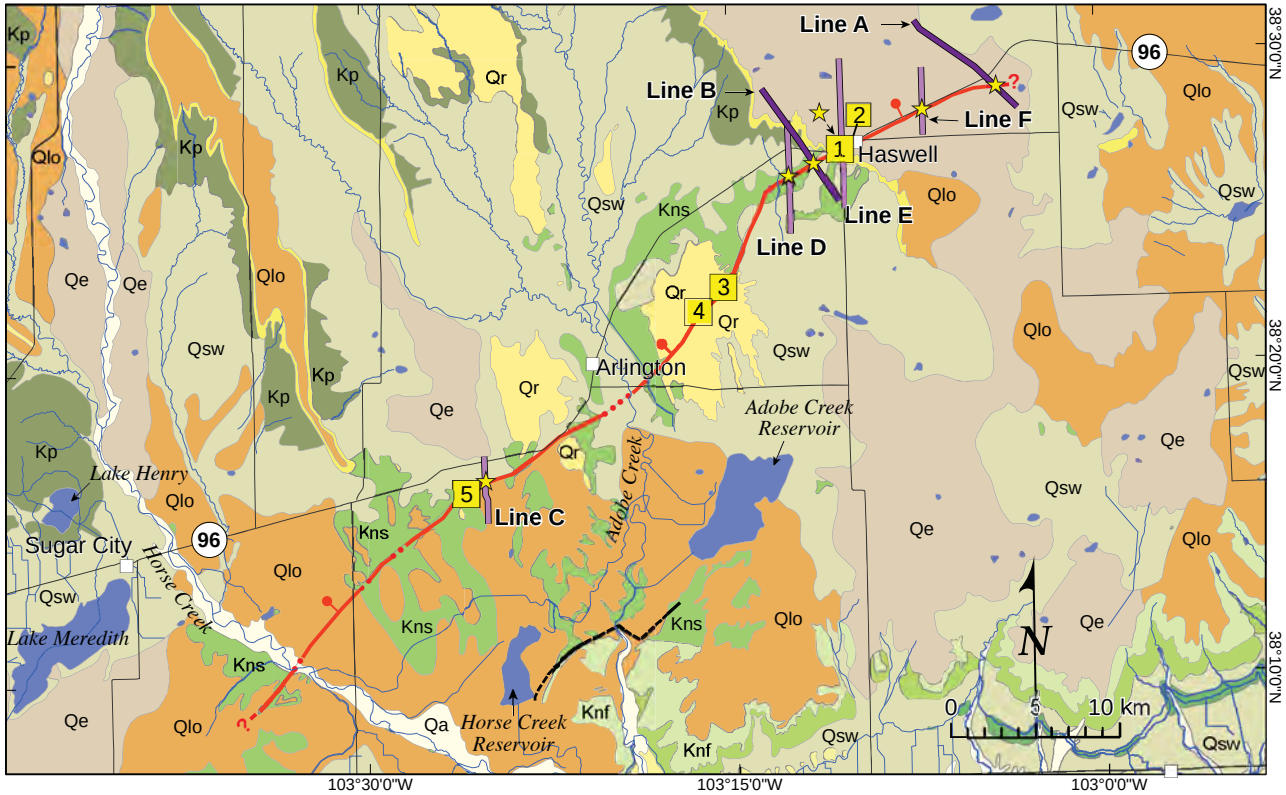

Geology modified from Sharps (1976)

Explanation

Correlation of Map Units

QUATERNARY

HOLOCENE

- Qa — Alluvium undiff.
- Qe — Eolian sand
- Qsw — Slopewash
- Qlo — Loess

PLESITOCENE

- Qr — Rocky flats alluvium
- Qn — Nussbaum alluvium

Unconformity

CRETACEOUS

- Kp — Pierre Shale
- Kns — Niobrara Fm., Smokey Hills mbr.
- Knf — Niobrara Fm., Fort Hayes mbr.
- Kc — Carlile Shale
- Kg — Greenhorn Limestone
- Water

Symbols

- Interpreted fault location
- Cheraw fault; dotted where concealed, dashed where topgraphic scarp absent, barb on downthrown side
- Fault; dashed where uncertain
- Field site
- Contact

Industry Seismic Reflection

- Depth migrated
- Time domain

Field Site Key

- 1 Site 1: shallow seismic survey, outcrop mapping, boreholes (2015)
- 2 Site 2: shallow seismic survey, (2015)
- 3 Site 3: shallow seismic survey, (2015)
- 4 Shallow seismic survey, (2014)
- 5 Shallow seismic survey, (2014) USGS trench (1995)

B)

ERATHEM	SYSTEM	Series	Stratigraphic Units (* - unit contains oil and gas)	Dominant Lithology	Thickness (Feet)	
CENOZOIC	QUATERNARY	Holocene		Alluvium		
		Pleistocene		Alluvium and Eolian deposits		
	TERTIARY	Miocene	Ogallala Formation	Sand and gravel		
MESOZOIC	CRETACEOUS	Upper	Pierre Shale, Niobrara Fm., Carlile Shale, Greenhorn Ls., Graneros Shale (Kgr)	Shale and limestone	0-3,500	Laramide Orogeny
		Lower	Dakota Sandstone (Kd)	Sandstone and mudstone	0-350	
	JURASSIC	Upper	Morrison Fm., Ralston Cr. Fm. (part) (Jm)	Sandstone and mudstone	100-350	
		Middle	Ralston Cr. Fm. (part), Entrada Ss.			
	TRIASSIC	Upper	Dockum Group (Pb)	Sandstone, mudstone, limestone, and dolomite	0-500	
PALEOZOIC	PERMIAN	Guadalupian	Talega Fm., Day Creek Dol., Whitehorse Ss.	Mudstone, sandstone, conglomerate, and carbonate, and evaporitic rocks	1,400 - 3000	Ouchita-Marathon Orogeny
		Leonardian	Nippewalla Group, Summer Group			
		Wolfcampian	Chase Group, Council Grove Group, Admire Group			
	PENNSYLVANIAN	Virgilian	Washumsee Group, Shawnee Group*, Douglas Group	Carbonate rocks, shale, sandstone, and conglomerate	1,400 - 3000	
		Missourian	Lansing Group*, Kansas City Group*			
		Desmoinesian	Marmaton Group*, Cherokee Group* (Pm)			
		Atokan	(Pv) *			
		Morrowan	*			
	MISSISSIPPIAN	Meramecian	St. Genevieve Ls., St. Louis Fm.*, Salem Fm.*, Warsaw Fm.* (Msg)	Carbonate rocks and mudstone	0 - 600	
		Osagean	Harrison Shale, St. Joseph Fm.*			
		Kinderhookian	Gilmore City Ls. equivalent, Misener Sand			
	ORDOVICIAN	Lower	Arbuckle Group	Dolomite and limestone	150 - 450	
	CAMBRIAN	Upper	Reagan Sandstone	Sandstone	0 - 100	
PRECAMBRIAN			Metamorphic and igneous rocks			

Modified from Meriwether, 1987.

Figure 4. Geologic Map and Stratigraphy

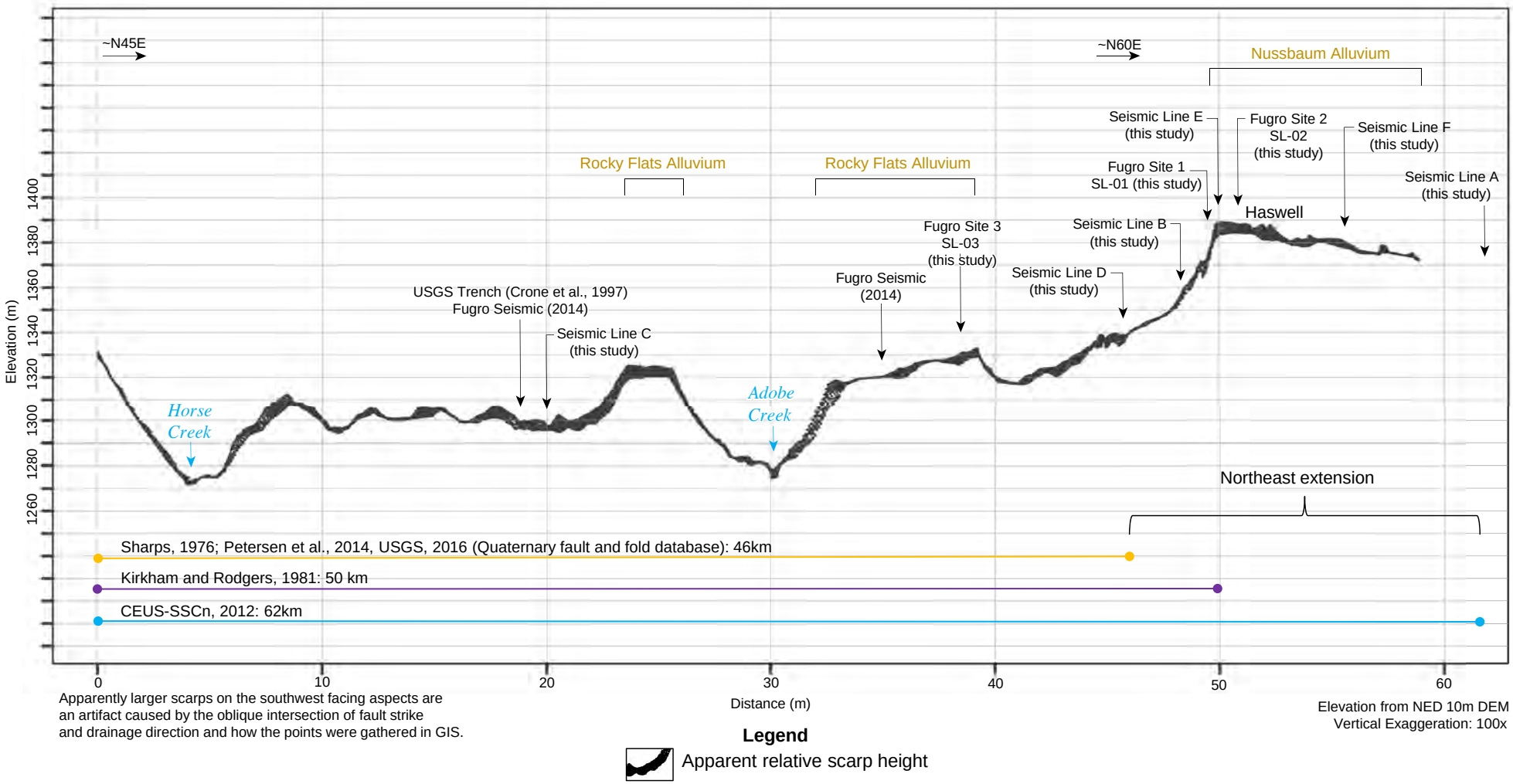

Figure 5. Along-strike Scarp Profile

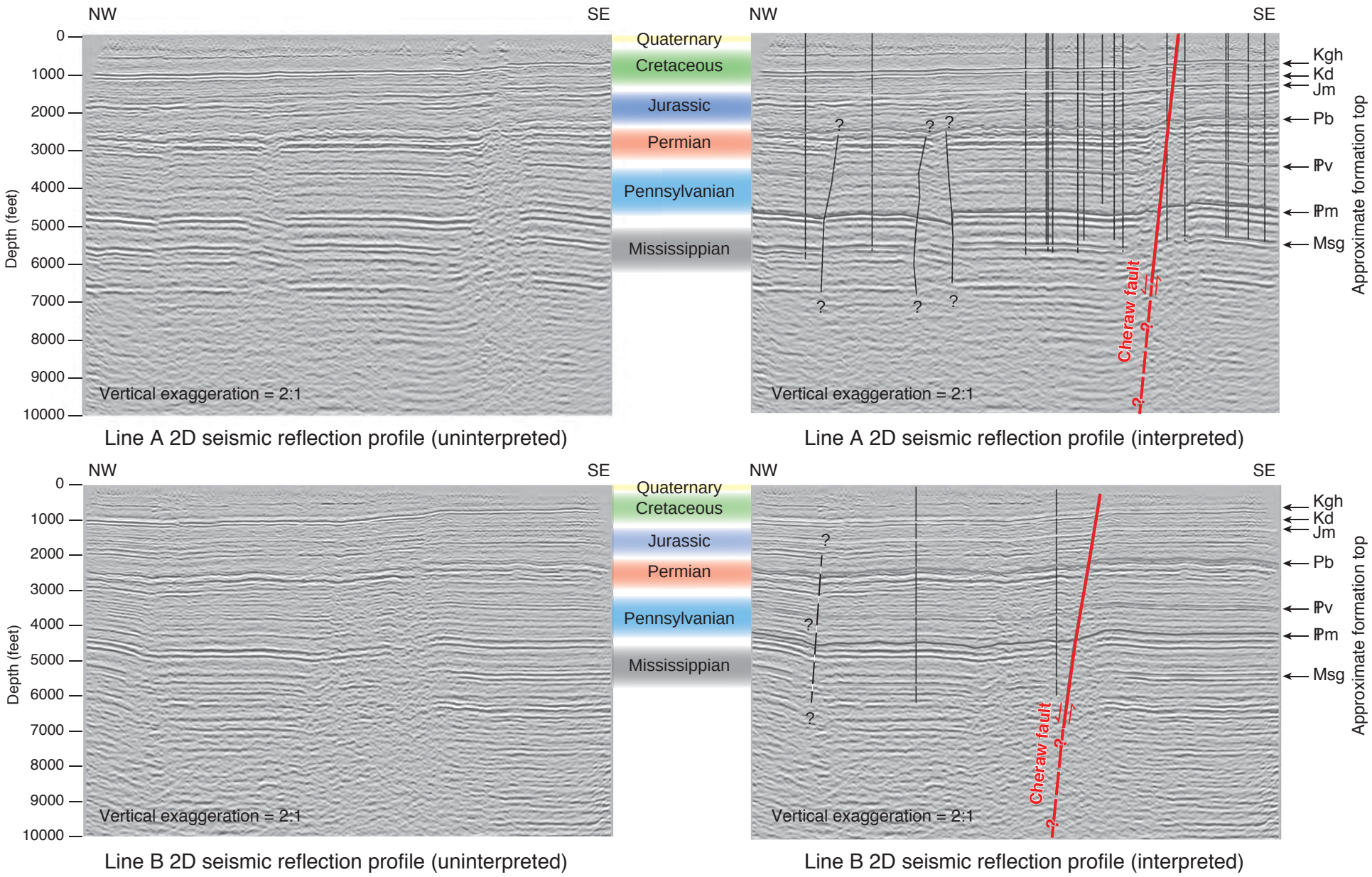

Figure 6. Lines A and B: 2D Depth Domain Seismic Reflection Profiles

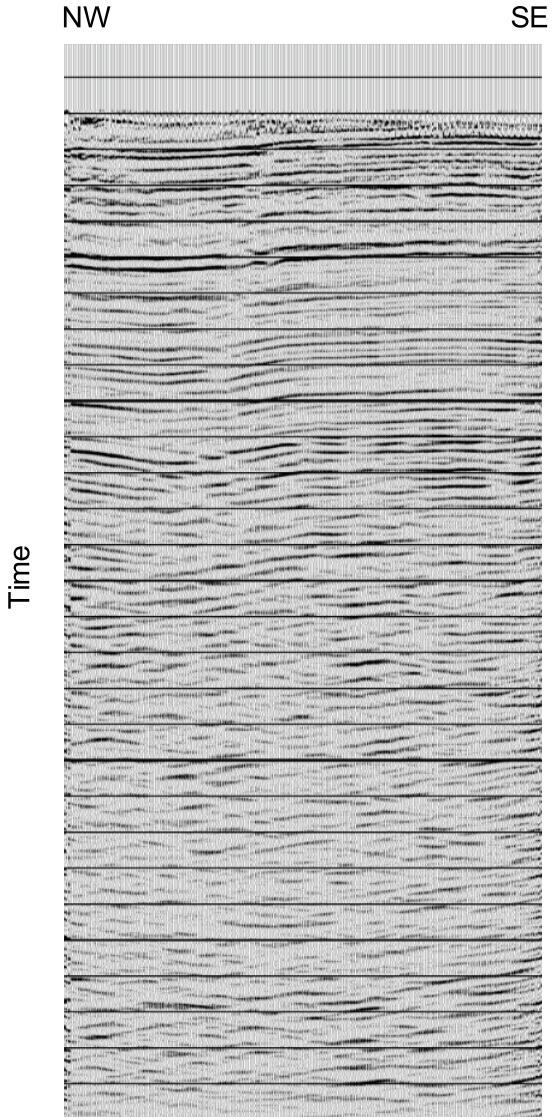

Uninterpreted

Seismic data owned or controlled by Seismic Exchange, Inc.; interpretation is that of Fugro Consultants, Inc.

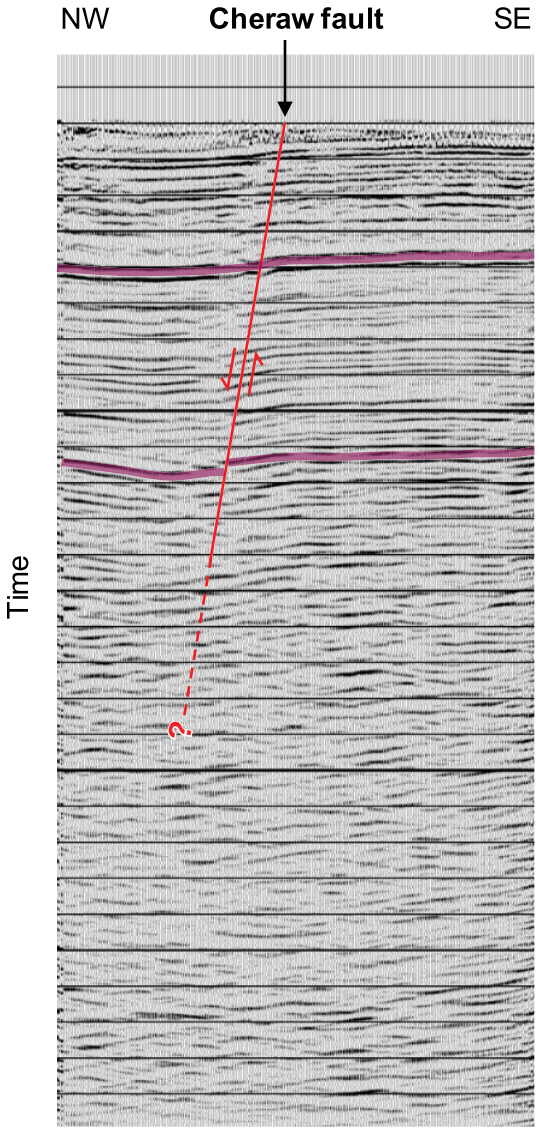

Interpreted

Arbitrary reflectors highlighted for reference. Location of Cheraw fault is approximate

Figure 7. Line C: 2D Time Domain Seismic Profile

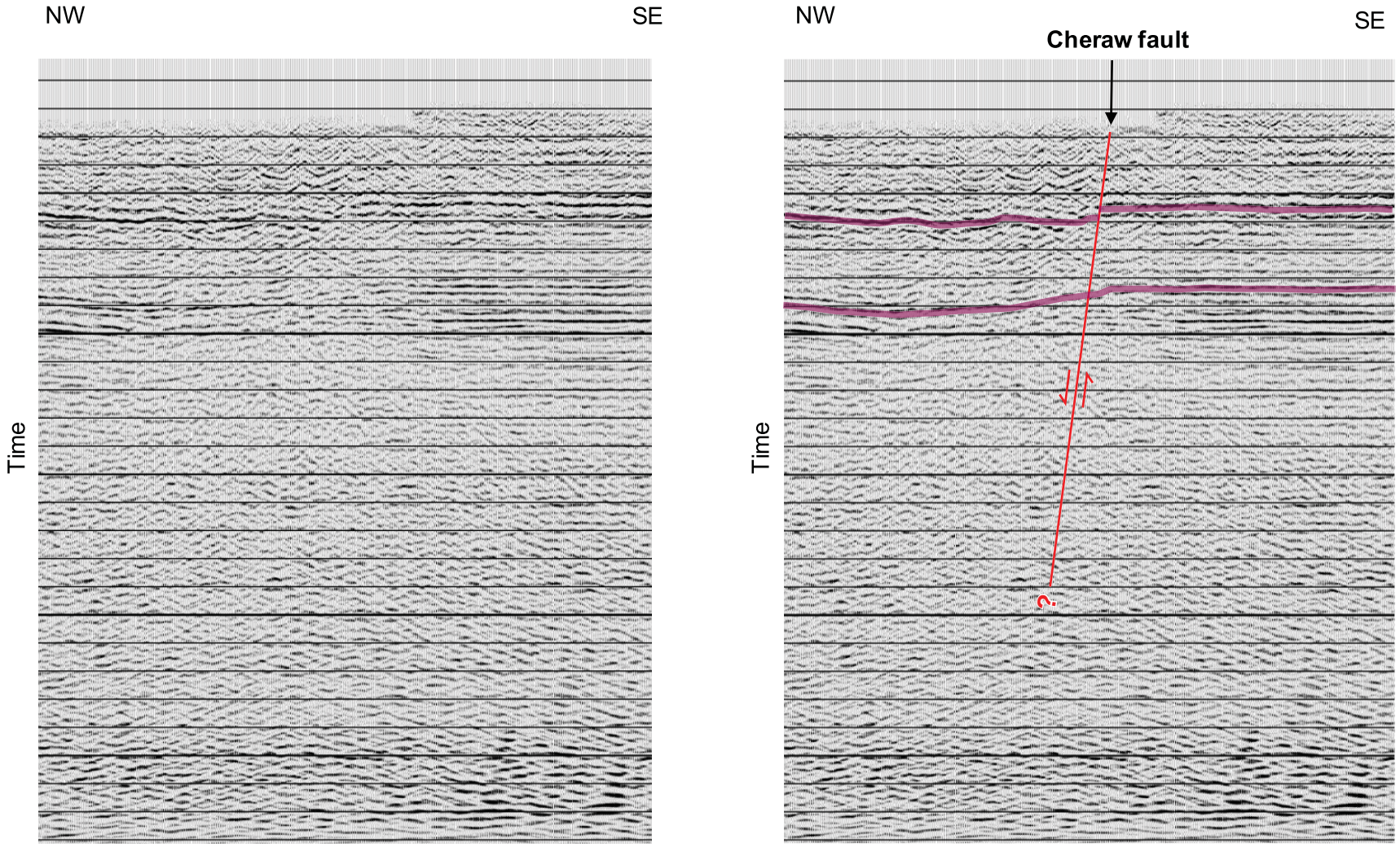

Uninterpreted

Interpreted

Seismic data owned or controlled by Seismic Exchange, Inc.; interpretation is that of Fugro Consultants, Inc.

Arbitrary reflectors highlighted for reference. Location of Cheraw fault is approximate

Figure 8. Line D: 2D Time Domain Seismic Profile

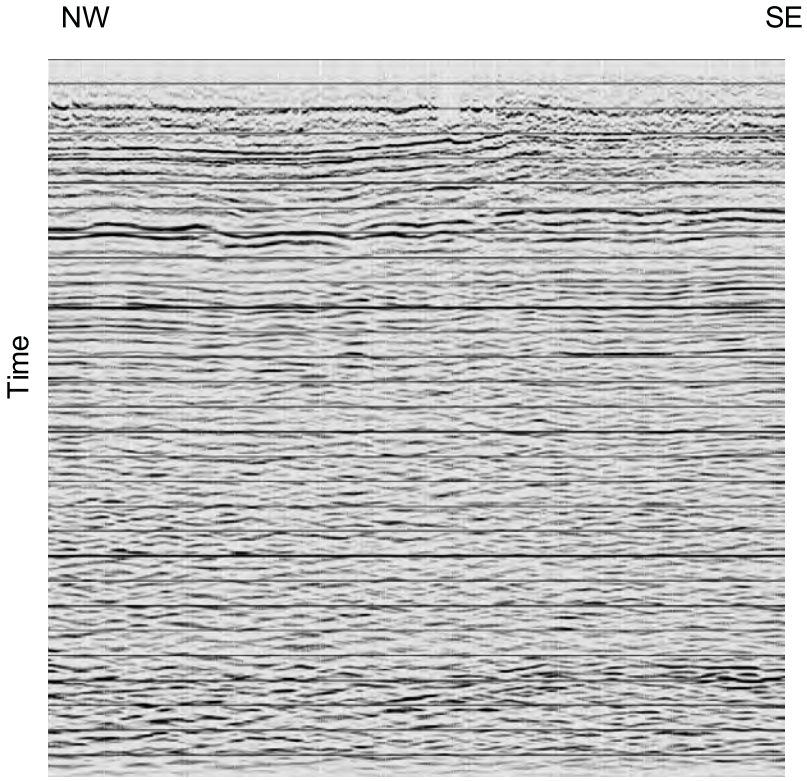

Uninterpreted

Seismic data owned or controlled by Seismic Exchange, Inc.; interpretation is that of Fugro Consultants, Inc.

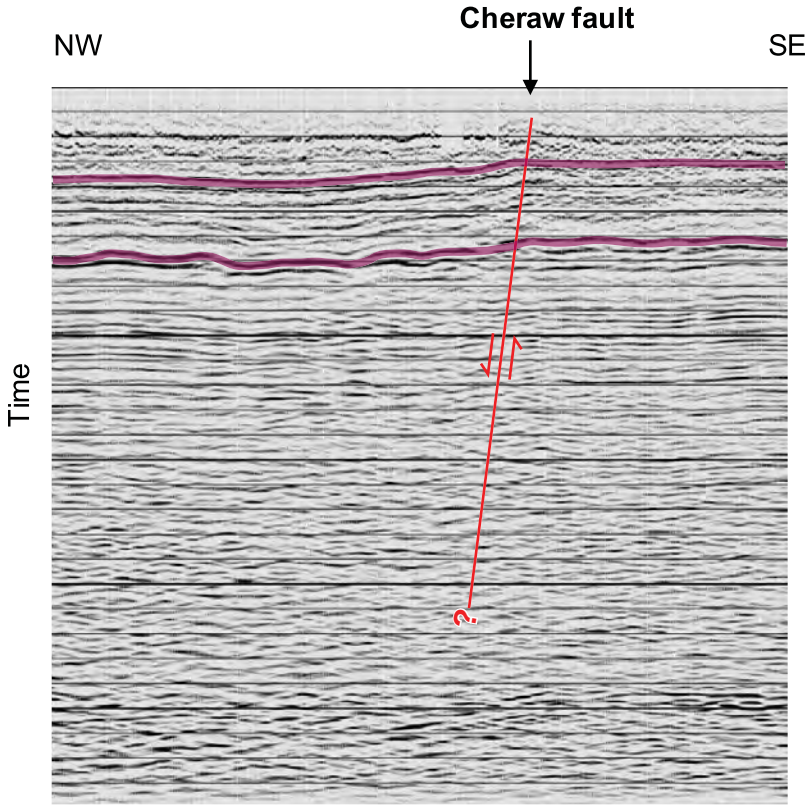

Interpreted

Arbitrary reflectors highlighted for reference.
Location of Cheraw fault is approximate

Figure 9. Line E: 2D Time Domain Seismic Profile

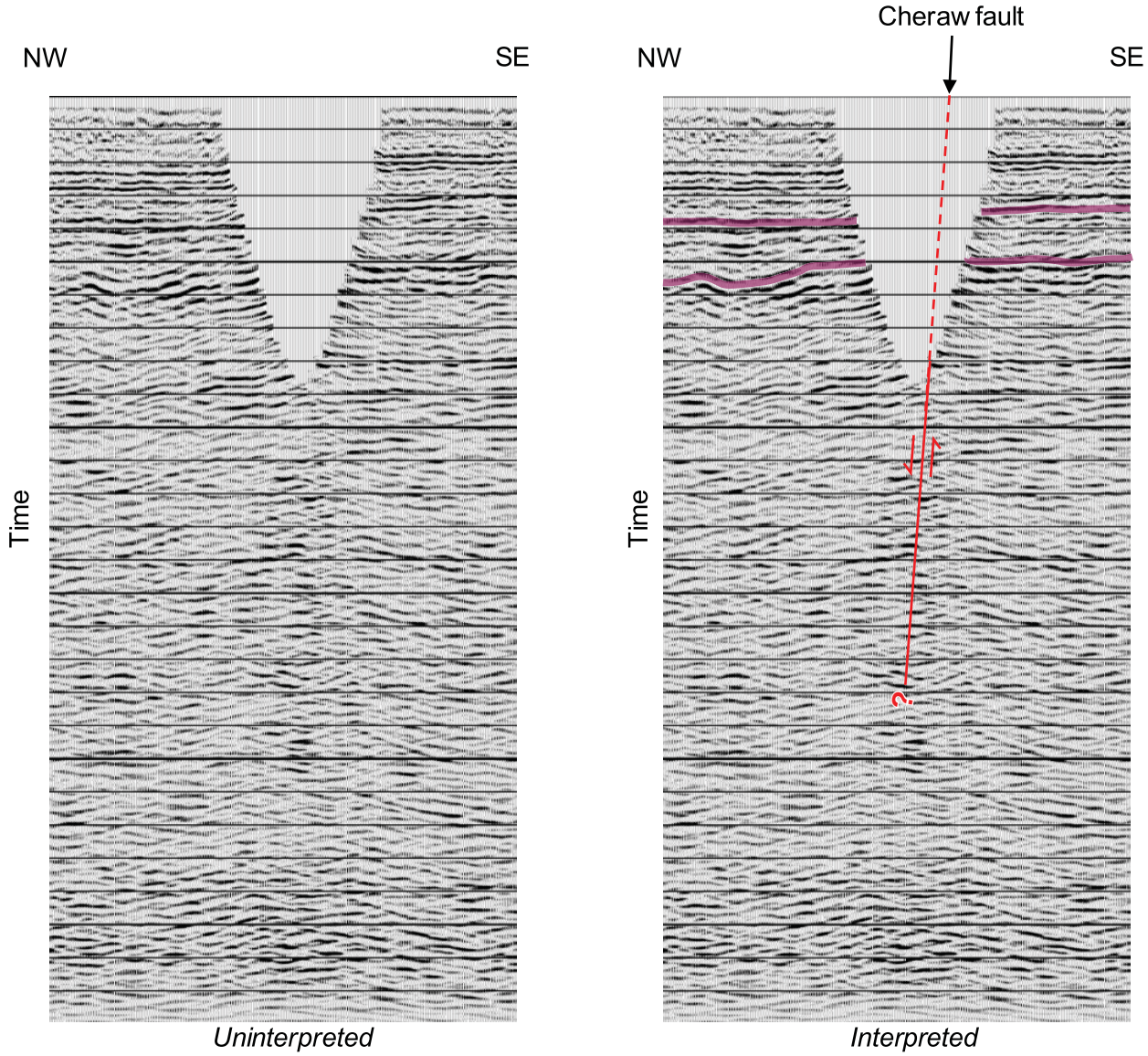

Seismic data owned or controlled by Seismic Exchange, Inc.; interpretation is that of Fugro Consultants, Inc.

Arbitrary reflectors highlighted for reference. Location of Cheraw fault is approximate

Figure 10. Line F: 2D Time Domain Seismic Profile

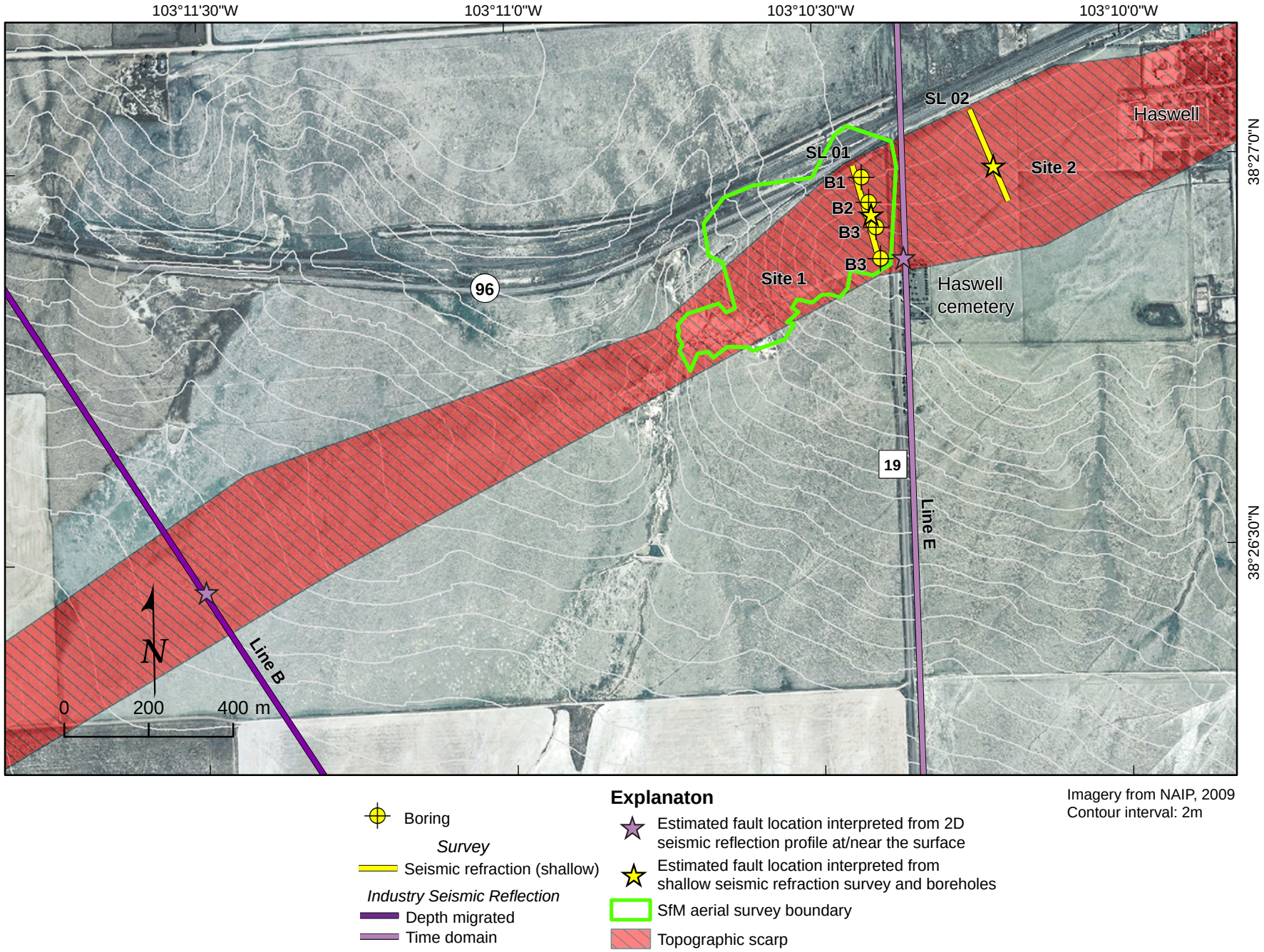

Figure 11. Haswell Area Site 1 and Site 2 Investigation

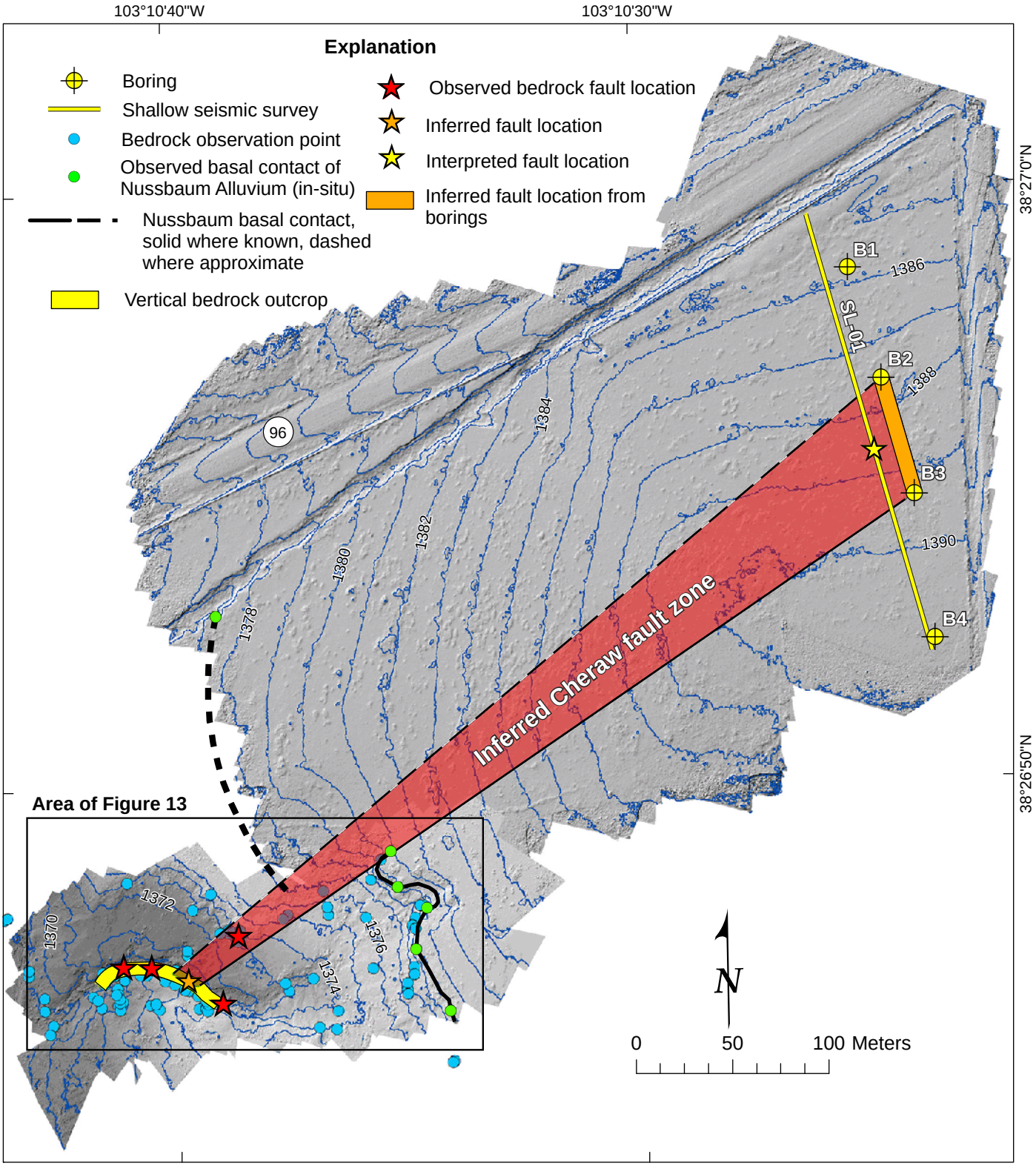

DEM from SFM (this study). Contour interval 1m.

Figure 12. Site 1 Fault Interpretation

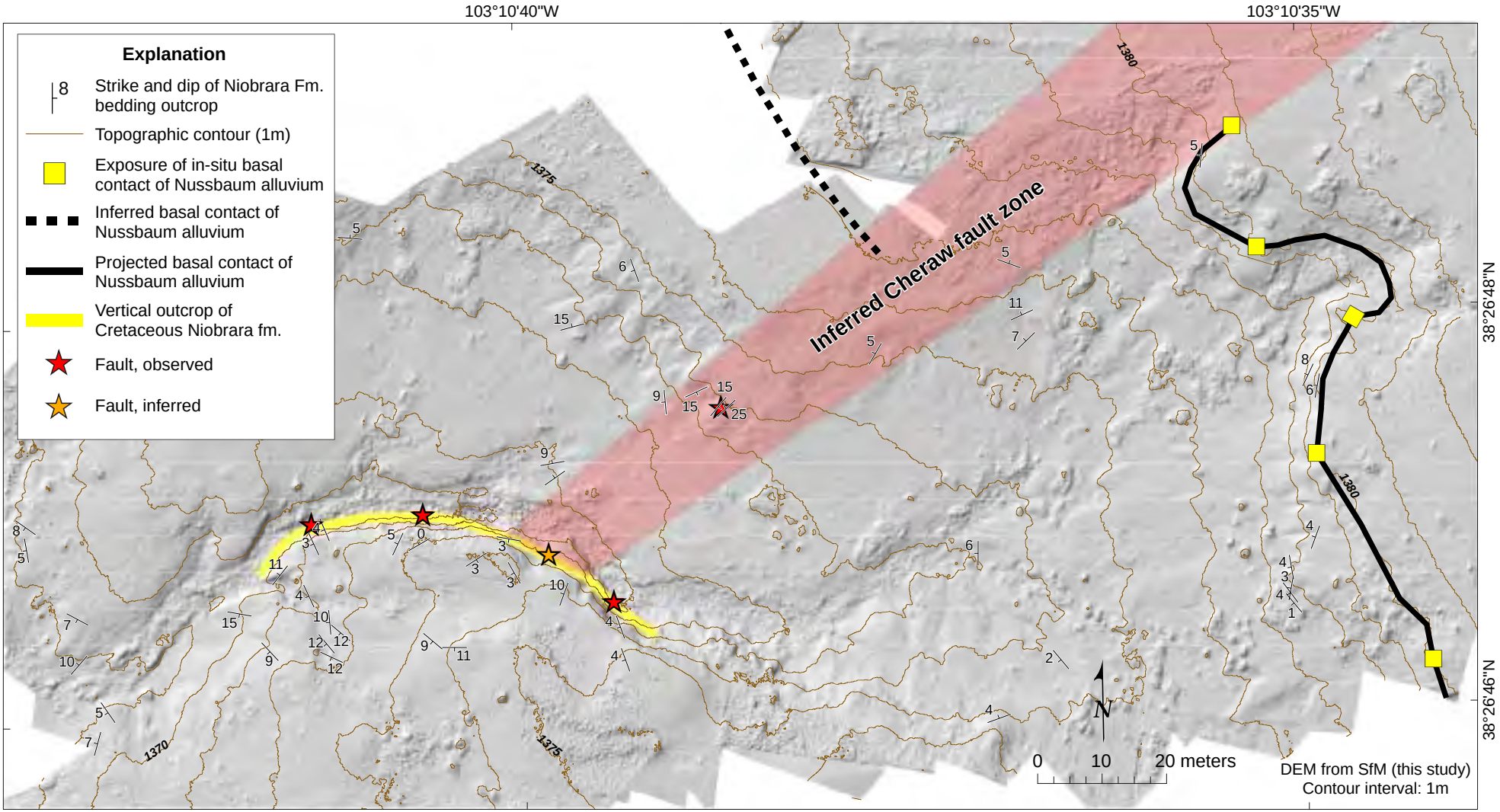

Figure 13. Site 1 Structural Map

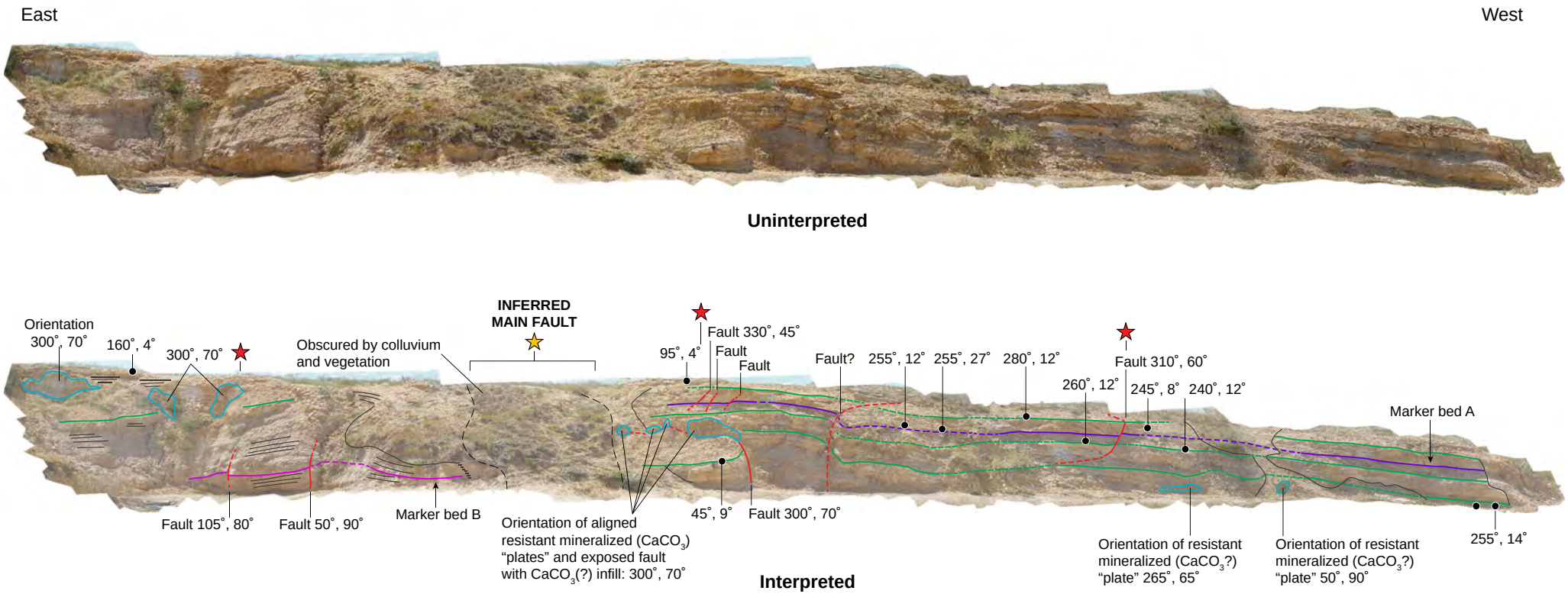

Explanation

- Marker bed A, dashed where uncertain
- Marker bed B, dashed where uncertain
- Mineralization
- Fault, dashed where uncertain
- Top of bed, dashed where uncertain
- Bedding
- Fault, observed
- Fault, inferred

Figure 14. Site 1 Outcrop Map

Figure 15. Photograph of Contact between Nussbaum Alluvium (Qn) and Niobrara Formation (Kns)

Photograph looking southeast at the unconformable contact between early (?) Quaternary Nussbaum Alluvium (Qn) and Cretaceous Smoky Hill member of Niobrara fm. (Kns) exposed in a ditch adjacent to Highway 96 at Site 1. The contact is planar and horizontal. The apparent dip to the right is caused by the angle of the photograph. This contact at this location is ~3m lower than an exposure of the same contact ~200 m to the south on the footwall of the Cheraw fault (Figure 12).

Figure 16. Photograph of Faulted Bedrock

Photograph looking northeast at an excavated exposure of faulted bedrock. Beds on the left dip ~15° to the southeast, and beds on the right dip ~ 25° to the northwest. This location is shown in Figure 12 as a red star within the inferred Cheraw fault zone.

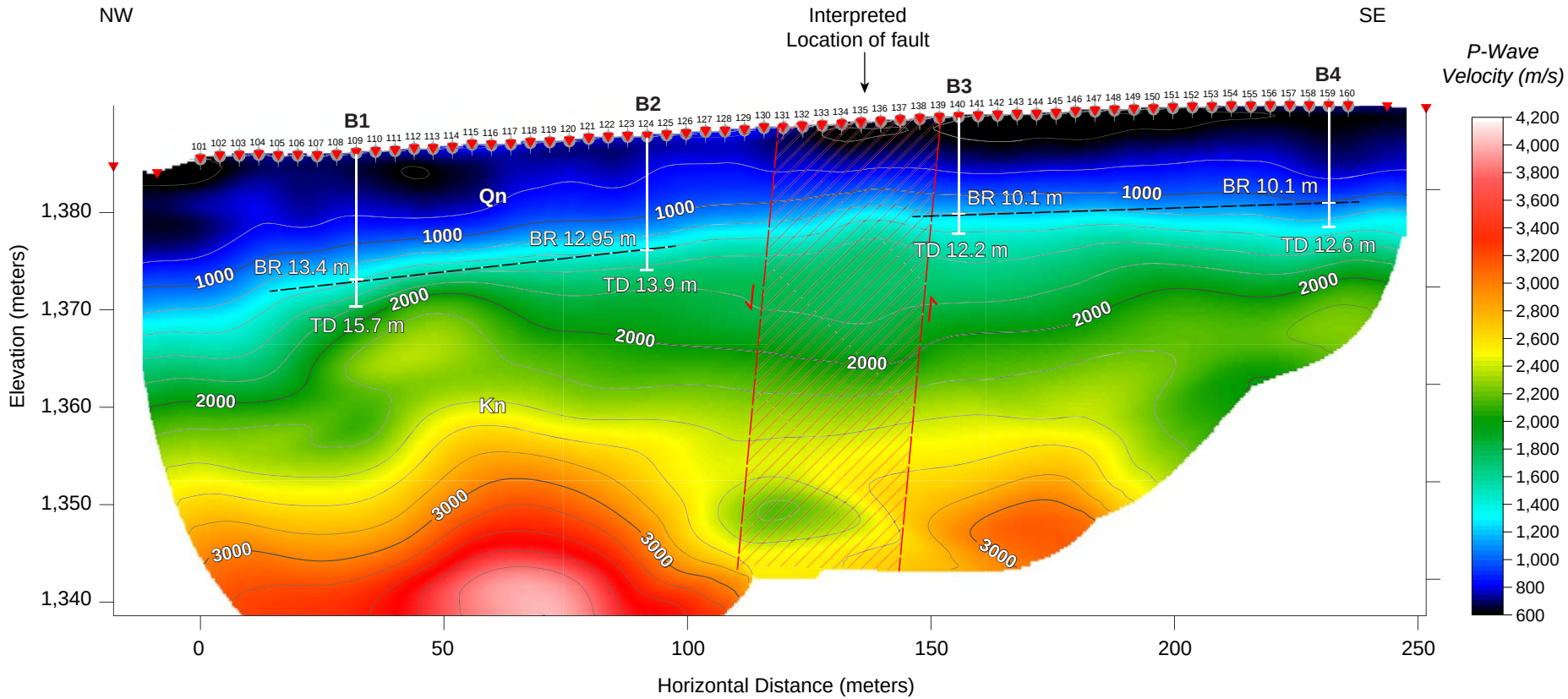

See Figures 4 and 12 for location.

Explanation

Shot location

123 Receiver station

Alluvium-bedrock contact, interpreted from boreholes

Figure 17. Site 1 Shallow Seismic Refraction Survey Profile SL-01

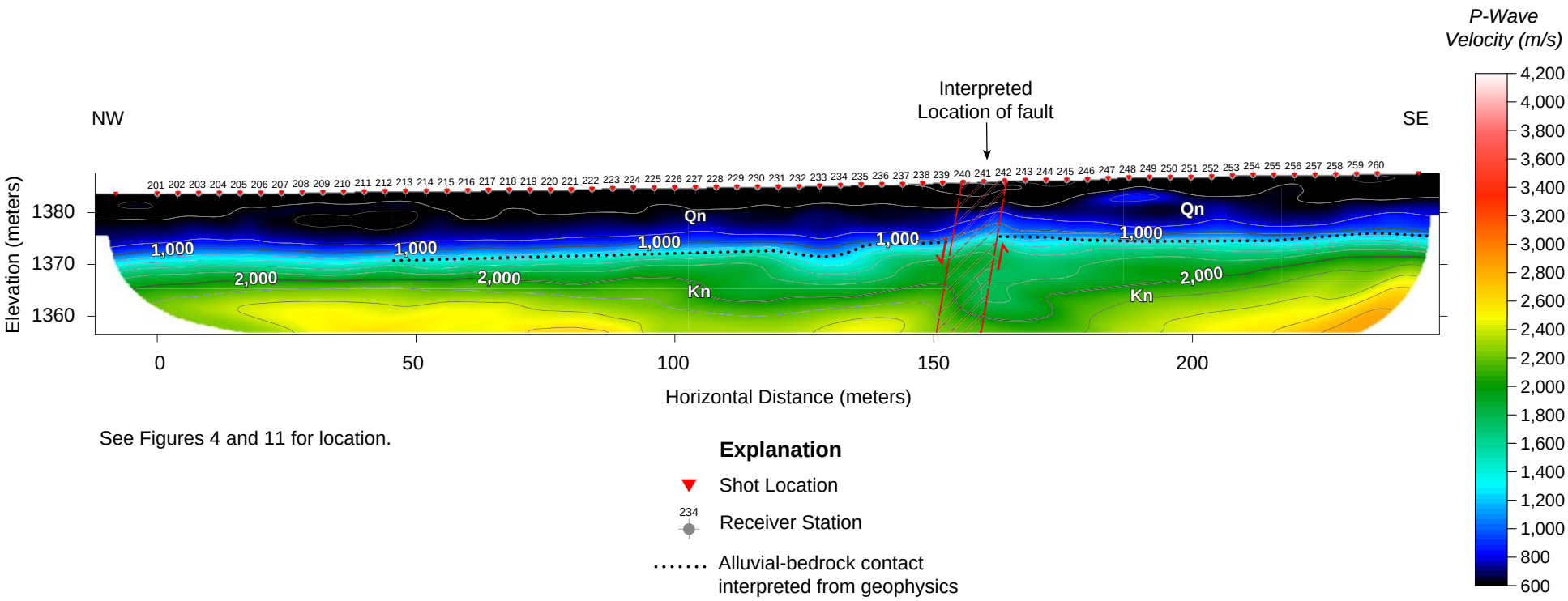

See Figures 4 and 11 for location.

Explanation

Shot Location

234 Receiver Station

Alluvial-bedrock contact interpreted from geophysics

Figure 18. Site 2 Shallow Seismic Refraction Survey Profile SL-02

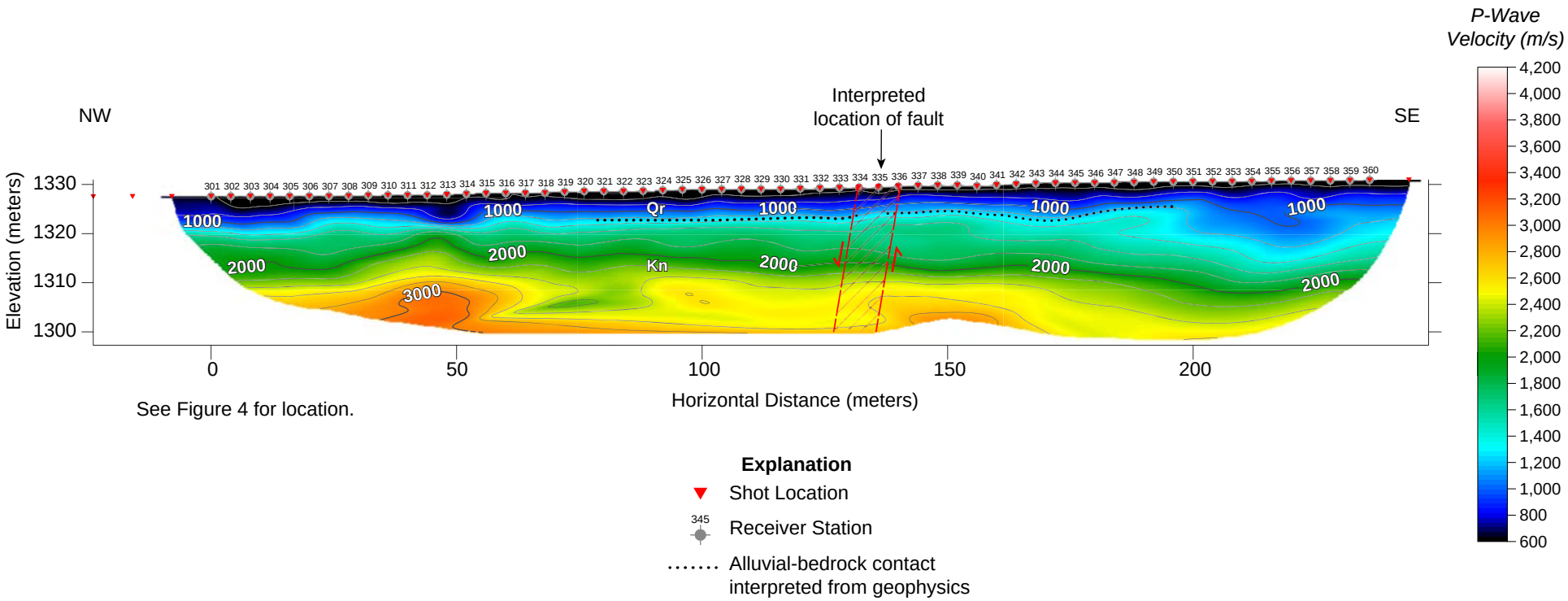

Figure 19. Site 3 Shallow Seismic Refraction Survey Profile SL-03